

(2)

AD-A153 922

TARGET MOTION ANALYSIS ALGORITHMS FOR
RAPID LOCALIZATION METHODS

DTIC
ELECTE
MAY 9 1985
B

DTIC FILE COPY

DISTRIBUTION STATEMENT A
Approved for public release
Distribution Unlimited

MANDEX, INC.

85 04 11 044

TARGET MOTION ANALYSIS ALGORITHMS FOR RAPID LOCALIZATION METHODS

Technical Report by Jim B. McQuitty

27 February 1985

Prepared under Contract N60921-84-C-0098

For:

Naval Surface Weapons Center
White Oak Laboratory
Silver Spring, MD 20903-5000
Code U-21 (Malcolm M. Coate)



Approved By:

Daniel D. Woolston

Daniel D. Woolston
Group Vice President

REPRODUCTION IN WHOLE OR IN PART
IS PERMITTED FOR ANY PURPOSE
OF THE UNITED STATES GOVERNMENT

APPROVED FOR PUBLIC RELEASE:
DISTRIBUTION UNLIMITED

REPORT DOCUMENTATION PAGE		READ INSTRUCTIONS BEFORE COMPLETING FORM
1. REPORT NUMBER	2. GOVT ACCESSION NO.	3. RECIPIENT'S CATALOG NUMBER
	AD-A153922	
4. TITLE (and Subtitle) Target Motion Analysis Algorithms for Rapid Localization Methods		5. TYPE OF REPORT & PERIOD COVERED Final Report
		6. PERFORMING ORG. REPORT NUMBER
7. AUTHOR(s) Jim B. McQuitty		8. CONTRACT OR GRANT NUMBER(s) N60921-84-C-0098
9. PERFORMING ORGANIZATION NAME AND ADDRESS Mandex, Inc./Underwater Systems Group 1776 E. Jefferson Street, Suite 322S Rockville, MD 20852		10. PROGRAM ELEMENT, PROJECT, TASK AREA & WORK UNIT NUMBERS
11. CONTROLLING OFFICE NAME AND ADDRESS Naval Surface Weapons Center White Oak Laboratory Silver Spring, MD 20910		12. REPORT DATE 27 February 1985
		13. NUMBER OF PAGES 55
14. MONITORING AGENCY NAME & ADDRESS (if different from Controlling Office)		15. SECURITY CLASS. (of this report) UNCLASSIFIED
		15a. DECLASSIFICATION/DOWNGRADING SCHEDULE
16. DISTRIBUTION STATEMENT (of this Report) Approved for public release; distribution is unlimited.		
17. DISTRIBUTION STATEMENT (of the abstract entered in Block 20, if different from Report)		
18. SUPPLEMENTARY NOTES		
19. KEY WORDS (Continue on reverse side if necessary and identify by block number) Range-Bearing TMA, TMA Error Analysis, Rapid Localization, Wide Aperture Array, Underwater Fire Control, Bearings-Only TMA, Least-Squares Linear Regression TMA		
20. ABSTRACT (Continue on reverse side if necessary and identify by block number) Several least-squares linear regression Target Motion Analysis (TMA) algorithms were derived for use when target range as well as bearing measurements are available from Rapid Localization (RAPLOC) underwater passive acoustic sensor systems, including the Wide Aperture Array (WAA) for attack submarines. Simulation error analyses, for a number of typical target encounter geometries, -> Cont'd.		

Item 20 - Abstract - Continued

✓ were conducted for each of the range-bearing TMA algorithms and for the bearings-only TMA algorithm, which must be used whenever range data is unavailable. The results showed that one particular algorithm, $[K_{OPT}(R - B) + (B - O)]$, was significantly more accurate than any of the others against non-maneuvering targets and another algorithm, $(2, 2 \times 2; R - B)$, performed best against maneuvering targets. Both of these TMA algorithms require range as well as bearing measurement inputs. The optimum weighting factor, K_{OPT} , and weighting coefficient, α , which minimize the TMA errors were also derived.

Least-squares TMA algorithms were derived for the special case that the target's down-range velocity component is either known or assumed to be known. One of these is the least-squares linear regression algorithm for the Ekelund ranging method.

*add this to report on accuracy,
in document for later*

List of Figures

<u>Figure No.</u>		<u>Page</u>
2-1	TMA Geometry.	2-2
3-1	Typical Run Geometries Used For TMA Algorithm Comparisons	3-3
3-2	$\sigma(R)$ Versus K	3-5
3-3	$\sigma(R)$, $\sigma(V_R)$ and $\sigma(V_{CR})$ Versus K	3-6
3-4	Run Geometries Used to Analyze the Geometric Weighting Factor, α_g	3-9
3-5	$\sigma(R)$ and $RMS(R)$ Versus Geometric Weighting Factor, α_g . . .	3-12
3-6	Maneuvering Target Run Geometries Used For TMA Error Analysis.	3-13
3-7	TMA Errors Versus K For Maneuvering Target Runs	3-17
A-1	Geometry for D/E or Multipath Ranging	A-2
A-2	K_{OPT} Versus Range and Ocean Depth	A-4
B-1	Platform Target Encounter Tactics	B-3
B-2	Relative $\sigma(R)$ Versus Prediction Time.	B-4

List of Tables

<u>Table No.</u>		<u>Page</u>
3-1	Maneuvering Target Results.	3-15

CHAPTER 1
INTRODUCTION AND OBJECTIVES

The development of passive acoustic systems which can measure target range both rapidly and continuously, after detection and tracking have been achieved, has produced a requirement for the derivation and development of Target Motion Analysis (TMA) algorithms which can utilize both target range and bearing data. These TMA algorithms are used in Fire Control Systems (FCS) of submarines and surface warships. Their primary purpose is to localize, as a function of time, threat submarine targets in order to facilitate weapon aim, acquisition and target kill, and to avoid being counter-killed by target launched weapons. This requires TMA algorithm solutions at long standoff ranges which are both timely and accurate against targets that may maneuver frequently in an unpredictable manner. Such accuracy and timeliness can only be achieved with accurate rapid range and bearing data as inputs to the TMA algorithm. However, since there are rigorous constraints upon the range and bearing accuracies which can be achieved with even the best platform mounted sensor systems, it is important that only the most accurate TMA algorithms be developed and implemented into the FCSs of submarines and surface warships.

An objective of this study is to derive candidate TMA algorithms and compare their relative accuracies for typical encounter geometries, which include both maneuvering and non-maneuvering targets. A further objective of this study is to derive, for each candidate TMA algorithm, the optimum weighting coefficient for each range and bearing measurement versus time and, where applicable, the optimum weighting of the set of range measurements relative to the set of bearing measurements.

Most of the candidate TMA algorithms have previously been derived. Some have been implemented and tested with field test data. Although the bearings-only TMA algorithm has previously been error analyzed, none of those using both range and bearing data inputs has ever been adequately error analyzed.¹ Therefore, it has previously been impossible to quantify and compare their accuracies.

All recursive type TMA algorithms, such as the various Kalman filters, were rejected as candidate algorithms since they are all inherently less accurate than their least-squares linear-regression counterparts which are non-recursive (or batch) type TMA algorithms. Recursive type TMA algorithms also tend to be unstable, whereas the non-recursive type TMA algorithms are inherently stable.

The error analyses showed that one of the TMA algorithms was more accurate than any of the others for all of the non-maneuvering target encounter geometries, and it was almost as accurate as any of the others for those maneuvering target encounter geometries which were tested. This algorithm, called the $[K_{OPT} (R - B) + (B - O)]$ TMA algorithm, requires a reasonable estimate of the standard deviation range and bearing measurement errors in order to determine the value of the weighting factor, K_{OPT} . The results, conclusions and recommendations in this report should be of particular value to the developers and the users of underwater FCS for submarines and surface warships.

¹McQuitty, J. B. and Gold, B. A., Error Analysis of Bearings-Only TMA, Naval Surface Weapons Center, NSWC TR 81-99, 6 May 1982.

CHAPTER 2

DERIVATIONS OF TMA ALGORITHMS

All TMA algorithms are based upon the assumption that the target moves at constant velocity (i.e., constant course and speed) during the solution time interval. Thus, the Cartesian coordinate components of the target velocity are constants, and the target position components at time t are given by the following two equations (see Figure 2-1).

$$\begin{aligned}
 U + t\dot{U} &= \hat{R} \cos \hat{B} + \hat{X} = \hat{R}\hat{C} + \hat{X} \\
 &= [R - E(R)][c - E(c)] + X - E(X) \\
 &= Rc + X - cE(R) - \hat{R}E(c) - E(X)
 \end{aligned} \tag{1}$$

$$U + t\dot{U} - Rc - X = -cE(R) + \hat{R}sE(B) - E(X)$$

$$\begin{aligned}
 W + t\dot{W} &= R \sin \hat{B} + \hat{Y} = \hat{R}\hat{S} + \hat{Y} \\
 &= [R - E(R)][s - E(s)] + Y - E(Y) \\
 &= Rs + Y - sE(R) - \hat{R}E(s) - E(Y)
 \end{aligned} \tag{2}$$

$$W + t\dot{W} - Rs - Y = -sE(R) - \hat{R}cE(B) - E(Y)$$

where

(U, W) are the initial target position components (at time $t = 0$)

(\dot{U}, \dot{W}) are the target velocity components

\hat{R} is the actual target range at time t

R is the measured target range at time t

$E(R)$ is the range error at time t

B is the measured target bearing at time t

(X, Y) are the measured platform position components at time t

$c = \cos B$; $E(c) = -sE(B)$

$s = \sin B$; $E(s) = cE(B)$

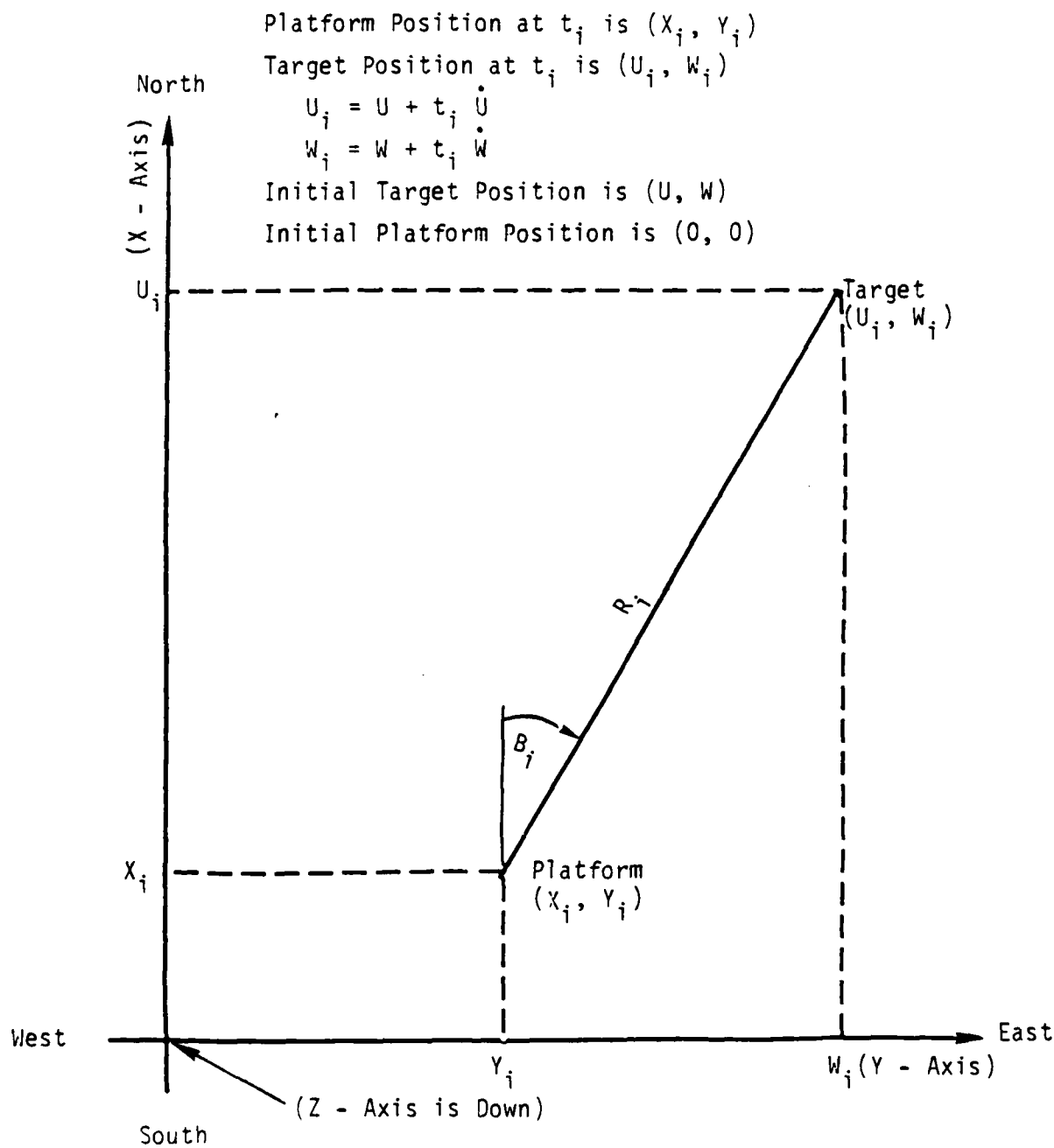


Figure 2-1. TMA Geometry.

2.1 THE (2, 2 x 2; R - B) TMA ALGORITHM

Two or more sets of (R, B, X, Y and t) measurements obtained at different times can be used to generate a set of simultaneous linear equations that can be used to solve for the four unknowns: U and \dot{U} , using Eq. (1), and W and \dot{W} , using Eq. (2). If the measurements of (R, B, X, Y and t) had no errors, any two sets of measurements, obtained at different times, would suffice to obtain an error-free solution. However, since these measurements invariably have errors, it is desirable to try to minimize their effect upon the solution accuracy. A reasonable assumption is that the measurement parameters (R, B, X, Y and t) are essentially independent and that each has random Gaussian-distributed zero-mean errors. If this assumption is valid, the least-squares linear-regression method, invented by Gauss, will give the most statistically accurate solution of the four unknowns (U, \dot{U} , W and \dot{W}). The first step in this method is to obtain a weighted sum of the squares of two sets of equations like Eqs. (1) and (2), respectively, as follows:

$$\sum_{i=1}^n \alpha_i (U + t \dot{U} - R_i - X_i)^2 = \sum_{i=1}^n \alpha_i [-cE(R) + \hat{R} sE(B) - E(X)]_i^2 = E_X^2 \quad (3)$$

$$\sum_{i=1}^n \alpha_i (W + t \dot{W} - R_i - Y_i)^2 = \sum_{i=1}^n \alpha_i [-sE(R) + \hat{R} cE(B) - E(Y)]_i^2 = E_Y^2 \quad (4)$$

The next step is to obtain the partial derivatives of Eqs. (3) and (4) with respect to the unknown parameters and set them equal to zero. This will give a minimum variance equation for each of the unknowns as follows:

$$\frac{\partial}{\partial U} \sum_{i=1}^n \alpha_i (U + t \dot{U} - R_i - X_i)^2 = 2 \sum_{i=1}^n \alpha_i (U + t \dot{U} - R_i - X_i) = 0 \quad (5)$$

$$\frac{\partial}{\partial \dot{U}} \sum_{i=1}^n \alpha_i (U + t \dot{U} - R_i - X_i)^2 = 2 \sum_{i=1}^n \alpha_i t_i (U + t \dot{U} - R_i - X_i) = 0 \quad (6)$$

$$\frac{\partial}{\partial W} \sum_{i=1}^n \alpha_i (W + t\dot{W} - R_s - Y)_i^2 = 2 \sum_{i=1}^n \alpha_i (W + t\dot{W} - R_s - Y)_i = 0 \quad (7)$$

$$\frac{\partial}{\partial \dot{W}} \sum_{i=1}^n \alpha_i (W + t\dot{W} - R_s - Y)_i^2 = 2 \sum_{i=1}^n \alpha_i t_i (W + t\dot{W} - R_s - Y)_i = 0 \quad (8)$$

Eqs. (5) and (6) can be put into the following matrix equation:

$$\begin{bmatrix} B_{11} & B_{12} \\ B_{12} & B_{22} \end{bmatrix} \cdot \begin{bmatrix} U \\ \dot{U} \end{bmatrix} = \begin{bmatrix} F_1 \\ F_2 \end{bmatrix} \quad (9a)$$

where

$$B_{11} = \sum \alpha = \sum_{i=1}^n \alpha_i$$

$$B_{12} = \sum \alpha t$$

$$B_{22} = \sum \alpha t^2$$

$$F_1 = \sum \alpha (R_c + X)$$

$$F_2 = \sum \alpha t (R_c + X)$$

Eqs. (7) and (8) in matrix form are

$$\begin{bmatrix} B_{11} & B_{12} \\ B_{12} & B_{22} \end{bmatrix} \cdot \begin{bmatrix} W \\ \dot{W} \end{bmatrix} = \begin{bmatrix} F_3 \\ F_4 \end{bmatrix} \quad (9b)$$

where

$$F_3 = \sum \alpha (R_s + Y)$$

$$F_4 = \sum \alpha t (R_s + Y)$$

Eqs. (9a) and (9b) comprise the (2, 2 x 2; R - B) TMA algorithm.

The sum of the squared errors in Eqs. (3) and (4), assuming that E(R), E(B), E(X) and E(Y) are independent zero-mean random errors, are respectively:

$$E_x^2 = \sum_{i=1}^n \alpha_i [c^2 E^2(R) + \hat{R}^2 s^2 E^2(B) + E^2(X)]_i \quad (10)$$

$$E_y^2 = \sum_{i=1}^n \alpha_i [s^2 E^2(R) + \hat{R}^2 c^2 E^2(B) + E^2(Y)]_i \quad (11)$$

Since these error squared terms are not known, the best we can do is to express them statistically in terms of their respective variance as follows:

$$\begin{aligned} \sigma^2(\text{TMA}) &= \frac{1}{m} \sum_{j=1}^m (E_x^2 + E_y^2); = \sigma_x^2(\text{TMA}) + \sigma_y^2(\text{TMA}) \\ &= \sum_{i=1}^n \alpha_i [\sigma^2(R) + \hat{R}^2 \sigma^2(B) + \sigma^2(X) + \sigma^2(Y)]_i \end{aligned} \quad (12)$$

This TMA solution variance, which is minimized by the linear regression algorithm, is the α weighted sum of the down-range variances, $\sum \alpha \sigma^2(R)$, the cross-range variances, $\sum \alpha \hat{R}^2 \sigma^2(B)$, and the platform position variances, $\sum \alpha [\sigma^2(X) + \sigma^2(Y)]$. Normally, the cross-range variance is much less than the down-range variance, especially at the longer ranges, since the cross-range error is proportional to range while the down-range error is proportional to range squared. This particular range-bearing TMA algorithm weights both of these errors equally, thus minimizing the down-range residual variance at the expense of the cross-range variance. The platform position variance is, also, small compared to the range variance, which leaves only the range variance as the dominant term in Eq. (12). This residual variance can be minimized even further by weighting each range measurement variance such that each of them is equal to the others. Let the weighting coefficient, α , be used for this equalization. Then,

$$\sigma^2(\text{TMA}) = \sum_{i=1}^n \alpha_i [\sigma^2(R) + R^2 \sigma^2(B) + \sigma^2(X) + \sigma^2(Y)]_i \approx \sum_{i=1}^n \alpha_i \sigma^2(R)_i \quad (13)$$

Each weighted range measurement variance term, $\alpha \sigma^2(R)$, is equal when α is inversely proportional to $\sigma^2(R)$. If the Wide Aperture Array (WAA) is used to measure target range, it can be shown that the range error is

$$\sigma(R) = \frac{CR^2 \sigma(\Delta\tau)}{L^2 \sin^2 \theta} \quad \text{since} \quad R = \frac{L^2 \sin^2 \theta}{C \Delta\tau} \quad (14)$$

where

C = speed of sound at the platform

L = separation between WAA subarrays

θ = relative target bearing

$\Delta\tau$ = time delay difference between the two target correlation signals at the WAA output

$\sigma(\Delta\tau)$ = standard deviation error in the $\Delta\tau$ measurement

R = target range

It can be shown that $\sigma(\tau)$, or $\sigma(\Delta\tau)$, is a function of the signal-to-noise at the input to the correlator processor.¹ The proposed signal-to-noise weighting of α due to $\sigma(\tau)$ or $\sigma(\Delta\tau)$ is the following:

$$\alpha_{S/N} = \left(\frac{2 S/N}{1 + 2 S/N} \right)^2 \quad (15)$$

The rationale for this weighting, instead of $\left(\frac{S}{N}\right)^2$ weighting, is due to the presence of random range and bearing measurement errors which are independent of signal-to-noise. These errors become the dominant errors whenever the signal-to-noise dependent errors become small (i.e., whenever the signal-to-

¹Ibid.

noise becomes large). Since the WAA correlator is a normalized processor, the height of the target correlation signal, which is a function of signal-to-noise at the input to the correlator, can be measured and used to calculate the signal-to-noise weighting factor, Eq. (15). Then, combining Eqs. (14) and (15) gives the following signal-to-noise and geometric weighting factors which will make α inversely proportional to $\sigma^2(R)$.

$$\alpha_i = (\alpha_{S/N})_i (\alpha_g)_i = \left(\frac{2 S/N}{1 + 2 S/N} \right)_i^2 \left(\frac{\sin^2 \theta}{R^2} \right)_i^2 \quad (16)$$

2.2 THE (4 x 4, R - B) TMA ALGORITHM

Eqs. (1) and (2) may be combined into a single equation which can be used to derive the (4 x 4, R - B) TMA algorithm. Multiply Eq. (1) by c and Eq. (2) by s and then add the two equations together to give

$$\begin{aligned} c(U + t\dot{U}) + s(W + t\dot{W}) &= R(\hat{c}c + \hat{s}s) + c\hat{X} + s\hat{Y} \\ &= R + cX + sY - E(R) - cE(X) - sE(Y) \\ c(U + t\dot{U}) + s(W + t\dot{W}) - (R + cX + sY) &= -E(R) - cE(X) - sE(Y) \end{aligned} \quad (17)$$

This is a single equation in the same four unknowns as in Eqs. (1) and (2), namely $(U, \dot{U}, W$ and $\dot{W})$. The least-squares linear regression solution of a set of n equations of this type, each for a different time, t_i , can be derived in the same manner as was used to derive Eqs. (5) through (9). The (4 x 4, R-B) TMA algorithm in matrix equation form is

$$\begin{bmatrix} A_{11} & A_{12} & A_{13} & A_{14} \\ A_{12} & A_{22} & A_{14} & A_{24} \\ A_{13} & A_{14} & A_{33} & A_{34} \\ A_{14} & A_{24} & A_{34} & A_{44} \end{bmatrix} \cdot \begin{bmatrix} U \\ \dot{U} \\ W \\ \dot{W} \end{bmatrix} = \begin{bmatrix} D_1 \\ D_2 \\ D_3 \\ D_4 \end{bmatrix} \quad (18)$$

where

$$A_{11} = \sum ac^2, A_{12} = \sum atc^2, A_{13} = \sum asc, A_{14} = \sum atsc$$

$$A_{22} = \sum at^2c^2, A_{24} = \sum at^2sc, A_{33} = \sum as^2, A_{34} = \sum ats^2$$

$$A_{44} = \sum at^2s^2$$

$$D_1 = \sum ac (R + cX + sY), D_2 = \sum atc (R + cX + sY)$$

$$D_3 = \sum as (R + cX + sY), D_4 = \sum ats (R + cX + sY)$$

The residual variance of this TMA algorithm as obtained from the random zero-mean errors on the righthand side of Eq. (17) is

$$\begin{aligned} \sigma^2(\text{TMA}) &= \frac{1}{m} \sum_{j=1}^m \sum_{i=1}^n \alpha_{ij} [E^2(R) + c^2E^2(X) + s^2E^2(Y)]_{ij} \\ &= \sum_{i=1}^n \alpha_i [\sigma^2(R) + c^2\sigma^2(X) + s^2\sigma^2(Y)] \\ &\approx \sum_{i=1}^n \alpha_i \sigma^2(R)_i, \end{aligned} \quad (19)$$

since the variance of the down-range component of platform position, $c^2\sigma^2(X) + s^2\sigma^2(Y)$, is small compared to the target range variance, $\sigma^2(R)$. Note the difference between this (4 x 4, R - B) TMA algorithm variance and that of the (2, 2 x 2; R - B) TMA algorithm, Eq. (13). There are only down-range error terms in Eq. (19), while Eq. (13) contains equally weighted down-range and cross-range components of platform position and target position error terms. Since the dominant error term is the same for Eq. (19) as for Eq. (13), the same weighting coefficient, α , given by Eq. (16), may be used with both the (4 x 4, R - B) and the (2, 2 x 2; R - B) TMA algorithms.

2.3 THE BEARINGS-ONLY, (B - 0), TMA ALGORITHM

Eqs. (1) and (2) may also be combined into a single equation which can be used to derive the bearings-only TMA algorithm. Multiply Eq. (1) by s ($= \sin B$) and multiply Eq. (2) by c ($= \cos B$). Then subtract Eq. (2) from Eq. (1) to give the following equation:

$$\begin{aligned} s(U + t\dot{U}) - c(W + t\dot{W}) - (sX - cY) &= \hat{R} (\hat{c}s - \hat{s}c) - sE(X) + cE(Y) \quad (20) \\ &= \hat{R}[c - E(c)] s - \hat{R}[s - E(s)] c - sE(X) + cE(Y) \\ &= \hat{R} E(B) - sE(X) + cE(Y) \end{aligned}$$

The least-squares linear-regression solution of a set of n equations of this type, each for a different time, t_i , can be derived in the same manner as was previously used to derive Eqs. (9) and (18). The bearings-only TMA algorithm becomes;

$$\begin{bmatrix} A_{33} & A_{34} & -A_{13} & -A_{14} \\ A_{34} & A_{44} & -A_{14} & -A_{24} \\ -A_{13} & -A_{14} & A_{11} & A_{12} \\ -A_{14} & -A_{24} & A_{12} & A_{22} \end{bmatrix} \cdot \begin{bmatrix} U \\ \dot{U} \\ W \\ \dot{W} \end{bmatrix} = \begin{bmatrix} E_1 \\ E_2 \\ E_3 \\ E_4 \end{bmatrix} \quad (21)$$

where the A 's are the same as those used in Eq. (17) and where

$$\begin{aligned} E_1 &= \sum \alpha s (sX - cY), \quad E_2 = \sum \alpha t s (sX - cY) \\ E_3 &= \sum \alpha c (cY - sX), \quad E_4 = \sum \alpha t c (cY - sX) \\ &= -\sum \alpha c (sX - cY), \quad = -\sum \alpha t c (sX - cY) \end{aligned}$$

The residual variance of this bearings-only TMA algorithm as obtained from the random, zero-mean errors (for $\alpha = 1$) on the right-hand side of Eq. (20) is

$$\begin{aligned} \sigma^2(\text{TMA}) &= \sum_{i=1}^n \alpha_i [\hat{R}^2 \sigma^2(B) + s^2 \sigma^2(X) + c^2 \sigma^2(Y)]_i \\ &\approx \sum_{i=1}^n \alpha_i R^2 \sigma^2(B), \end{aligned} \quad (22)$$

since the variance of the cross-range component of platform position, $s_{\sigma}^2(x) + c_{\sigma}^2(y)$, is assumed to be small compared to the target range variance. Note that this (B - 0) TMA algorithm variance has only cross-range error terms, as compared to the (4 x 4, R - B) TMA algorithm variance, Eq. (19), which has only down-range error terms. The weighting coefficient, α , which minimizes Eq. (22) is that for which each weighted cross-range variance term, $\alpha \hat{R}_{\sigma}^2(B)$ is equal to the others. Therefore, α must be inversely proportional to $\hat{R}_{\sigma}^2(B)$. The standard deviation bearing error, $\sigma(B)$, has the same signal-to-noise functional dependence as does $\sigma(\Delta\tau)$, so that the signal-to-noise weighting given by Eq. (15) may be used. Thus, the weighting coefficient for the (B - 0) TMA algorithm is

$$\alpha_i = \left(\frac{2 S/N}{1 + 2 S/N} \right)_i^2 \quad (23)$$

The (B - 0) TMA algorithm can be used when range measurements are unavailable, since only target bearing measurements are required for a valid solution. Without any range measurement data, the weighting coefficient reduces to the signal-to-noise weighting factor.

2.4 THE [K(R - B) + (B - 0)] TMA ALGORITHM

A weighted range-bearing and bearings-only TMA algorithm can be derived by adding a fraction, K, of the (4 x 4, R - B) TMA algorithm, Eq. (18), to the (B - 0) TMA algorithm, Eq. (21) as follows:

$$\begin{bmatrix} (KA_{11} + A_{33}) & (KA_{12} + A_{34}) & (K - 1)A_{13} & (K - 1)A_{14} \\ (KA_{12} + A_{34}) & (KA_{22} + A_{44}) & (K - 1)A_{14} & (K - 1)A_{24} \\ (K - 1)A_{13} & (K - 1)A_{14} & (KA_{33} + A_{11}) & (KA_{34} + A_{12}) \\ (K - 1)A_{14} & (K - 1)A_{24} & (KA_{34} + A_{12}) & (KA_{44} + A_{22}) \end{bmatrix} \cdot \begin{bmatrix} U \\ \dot{U} \\ W \\ \dot{W} \end{bmatrix} = \begin{bmatrix} (KD_1 + E_1) \\ (KD_2 + E_2) \\ (KD_3 + E_3) \\ (KD_4 + E_4) \end{bmatrix} \quad (24)$$

The rationale for this weighted range-bearing and bearings-only TMA algorithm is to provide an algorithm which minimizes the properly weighted sums of the down-range variance and the cross-range variance of the TMA solution. The variance of this algorithm is

$$\sigma^2 (\text{TMA}) = \sum_{i=1}^n \alpha_i [K\sigma^2(R) + \hat{R}^2\sigma^2(B) + (Kc^2 + s^2)\sigma^2(X) + (Ks^2 + c^2)\sigma^2(Y)]_i \quad (25)$$

This variance is a minimum when the weighted down-range variance sum is equal to the cross-range variance sum, or when

$$K_{\text{OPT}} = \frac{\sum \alpha [\hat{R}^2\sigma^2(B) + s^2\sigma^2(X) + c^2\sigma^2(Y)]}{\sum \alpha [\sigma^2(R) + c^2\sigma^2(X) + s^2\sigma^2(Y)]} \quad (26)$$

Note that the numerator is Eq. (22), the variance of the bearing-only TMA solution; and the denominator is Eq. (19), the variance of the range-bearing TMA solution. If the platform position variance is small relative to the target position variance, Eq. (26) reduces to the following:

$$K_{\text{OPT}} = \frac{\sum \alpha \hat{R}^2\sigma^2(B)}{\sum \alpha \sigma^2(R)} \approx \frac{\hat{R}^2\sigma^2(B)}{\sigma^2(R)} \quad (27)$$

If the WAA is used to measure range, $\sigma(R)$ is given by Eq. (14), and K is approximately the following:

$$K_{\text{OPT}} \approx \frac{\hat{R}^2\sigma^2(B) L^4 \sin^4 \theta}{C^2 R^4 \sigma^2(\Delta\tau)} \approx \left(\frac{L^2 \sin^2 \theta}{C R} \right)^2 \left(\frac{\sigma(B)}{\sigma(\Delta\tau)} \right)^2 \quad (28)$$

If $L = 86.6$ ft, $C = 5,000$ ft/sec, $R =$ kyds, $\sigma(B) =$ degrees and $\sigma(\Delta\tau) =$ microseconds, then

$$K_{\text{OPT}} \approx \left[\frac{8.75 \sin^2 \theta \sigma^2(B^\circ)}{R \sigma(\Delta\tau, \mu\text{sec})} \right]^2 = \left[0.175 \Delta\tau \frac{\sigma(B)}{\sigma(\Delta\tau)} \right]^2 \quad (29)$$

where

$$\bar{R} = \text{kyds}$$

$$\Delta\tau, \sigma(\Delta\tau) = \mu\text{sec}$$

$$\sigma(B) = \text{degrees}$$

Appendix A gives the K_{OPT} for D/E or multipath measurements.

The weighting coefficient, α , which minimizes Eq. (25), the σ^2 (TMA) for this algorithm, is obtained by first minimizing σ^2 (TMA) as a function of K by setting K equal to K_{OPT} as given in Eq. (27). This will make the first two variance terms in Eq. (25) equal to each other and if the other two (platform position) terms are comparatively small, Eq. (25) reduces to

$$\begin{aligned}\sigma^2 \text{ (TMA)} &\approx \sum \alpha_i [K_{OPT} \sigma^2(R) + \hat{R}^2 \sigma^2(B)]_i \\ &\approx 2 \sum [\alpha \hat{R}^2 \sigma^2(B)]_i\end{aligned}\tag{30}$$

If the bearing measurements are obtained from the WAA, the basic measurement is the time delay, τ , to the center of the target correlation signal. The relative target bearing as a function of τ is

$$\theta = \cos^{-1} \left(\frac{c\tau}{L} \right) \text{ or } \tau = \frac{L \cos \theta}{c}\tag{31}$$

where

L = baseline separation of the WAA subarrays

c = speed of sound in the water at the array

The relative target bearing error is

$$\sigma(\theta) = \frac{c \sigma(\tau)}{L \sin \theta}\tag{32}$$

If the platform heading error is assumed to be small compared to $\sigma(\theta)$, then $\sigma(\theta)$ is approximately equal to $\sigma(B)$, the true bearing error. Then, the weighting coefficient which minimizes Eq. (30) is inversely proportional to

the cross-range target position variance. Thus, the weighting coefficient for the $[K(R - B) + (B - 0)]$ TMA algorithm is

$$\alpha_i = \left(\frac{2 S/N}{1 + 2 S/N} \right)_i^2 \left(\frac{\sin \theta}{R} \right)_i^2 \quad (33)$$

Comparing this weighting coefficient with that for the $(2, 2 \times 2; R - B)$ and the $(4 \times 4, R - B)$ TMA algorithms, Eq. (16), shows that the geometric weighting for Eq. (33) is

$$\left(\frac{\sin \theta}{R} \right)^2$$

while for Eq. (16) it is the square of this or

$$\left(\frac{\sin \theta}{R} \right)^4$$

2.5 THE $(2 \times 2; R - B)$ TMA ALGORITHM FOR AN ASSUMED VALUE OF V_R

It is usually possible to obtain a more accurate TMA solution if the number of unknowns can be reduced from four to three. For example, if V_R can be directly calculated from the doppler frequency measurement of a target-radiated line-component whose frequency is exactly known, or if V_R is assumed to be known at any given time, t_k , the unknowns reduce to U , W and V_{CR} where

$$V_{CR} = V_{CR}(t = K) = -s_k \dot{U} + c_k \dot{W} \quad (34)$$

$$V_R = V_R(t = K) = c_k \dot{U} + s_k \dot{W}$$

$$\dot{U} = -s_k V_{CR} + c_k V_R \quad (35)$$

$$\dot{W} = c_k V_{CR} + s_k V_R$$

The TMA algorithm in matrix form is the following pair of equations:

$$\begin{bmatrix} B_{11} & B_{12} \\ B_{12} & B_{22} \end{bmatrix} \cdot \begin{bmatrix} U \\ -s_k V_{CR} \end{bmatrix} = \begin{bmatrix} (F_1 - c_k V_R B_{12}) \\ (F_2 - c_k V_R B_{22}) \end{bmatrix} \quad (36)$$

$$\begin{bmatrix} B_{11} & B_{12} \\ B_{12} & B_{22} \end{bmatrix} \cdot \begin{bmatrix} W \\ c_k V_{CR} \end{bmatrix} = \begin{bmatrix} (F_3 - s_k V_R B_{12}) \\ (F_4 - s_k V_R B_{22}) \end{bmatrix}$$

where the B_{ij} and the F_i are the same as those in Eq. (9). This TMA algorithm solves for four unknowns, U , W , and two values of V_{CR} . It can be reduced to only three unknowns by solving for the weighted mean of the two V_{CR} solutions.

$$V_{CR} = s_k (s_k V_{CR}) + c_k (c_k V_{CR}) = V_{CR} (t = t_k) \quad (37)$$

The value of V_R at time t_k is assumed to be known, and the solution for range, R , at time t_k is

$$\begin{aligned} \tilde{R}_K &= (c_k U + s_k W) + t_k V_R - (c_k X_K + s_k Y_K) \\ &= \tilde{R}_1 + t_k V_R - t_k \bar{R}_{\text{PLATFORM}} \end{aligned} \quad (38)$$

As previously mentioned, the range rate can be obtained by measuring the difference between the doppler-modified received frequency and the known radiated frequency as follows:

$$\dot{R}_K = (V_R - \dot{R}_{\text{PLATFORM}})_K = (V_R - V_p \cos \theta)_K = -3 \frac{\Delta f, \text{ Hz}}{f_0, \text{ kHz}}, \text{ knots} \quad (39)$$

where

V_p = platform speed

θ = relative target bearing

Solving this equation for V_R gives

$$V_R = (\dot{R} + V_p \cos \theta)_K \quad (40)$$

This algorithm can also be used when the target is in the convergence zone and is kept there all during the solution time by appropriate platform maneuvers. For this case, V_R at time t_k is assumed to be

$$V_R = \frac{c_k X_k + s_k Y_k}{t_k} \quad (41)$$

The solution for range, \tilde{R} , at time, t_k , from Eq. (38), reduces to

$$\tilde{R}_k = \tilde{R}_1 = c_k U + s_k W \quad (42)$$

Since the range is held almost constant by appropriate platform maneuvers, the accuracy of this range solution may be improved by solving for the median range. Whenever the median range measurement is used, the cross-range velocity solution, Eq. (37), should be modified as follows:

$$(V_{CR})_{MED} = \frac{\text{MEDIAN}(R)}{\tilde{R}_k} V_{CR} \quad (43)$$

The rationale for using the median range instead of the average range is due to the skewness of the range error distribution which can result in a large average range bias error, especially at the longer ranges, whereas the median range is statistically unbiased.

2.6 THE (B-0) TMA ALGORITHM FOR AN ASSUMED VALUE OF V_R

The bearings-only TMA set of equations in Cartesian coordinates is the following:

$$\sum_{i=1}^n [s_i (U + t_i \dot{U} - X_i) - c_i (W + t_i \dot{W} - Y_i)] = 0 \quad (44)$$

Changing the velocity components from Cartesian to polar geometry, using Eq. (35), and assuming that V_R is known, gives

$$\sum_{i=1}^n [s_i (U - t_i s_k V_{CR}) - c_i (W + t_i c_k V_{CR}) = (s_i X_i - c_i Y_i) - V_R t_i (s_i c_k - c_i s_k)] \quad (45)$$

The TMA algorithm in matrix form is

$$\begin{bmatrix} A_{33} & A_{34} & -A_{13} & -A_{14} \\ A_{34} & A_{44} & -A_{14} & -A_{24} \\ -A_{13} & -A_{14} & A_{11} & A_{12} \\ -A_{14} & -A_{24} & A_{12} & A_{22} \end{bmatrix} \cdot \begin{bmatrix} U \\ -s_k V_{CR} \\ W \\ c_k V_{CR} \end{bmatrix} = \begin{bmatrix} [E_1 - V_R (c_k A_{34} - s_k A_{14})] \\ [E_2 - V_R (c_k A_{44} - s_k A_{24})] \\ [E_3 + V_R (c_k A_{14} - s_k A_{12})] \\ [E_4 + V_R (c_k A_{24} - s_k A_{22})] \end{bmatrix} \quad (46)$$

where the A_{ij} and the E_i are the same as those in Eq. (21). This algorithm also solves for four unknowns, which can be reduced to only three unknowns by using Eq. (37) to solve for the weighted mean value of the two V_{CR} solutions. The solution (U , W and V_{CR}) plus the assumed known value of V_R can be converted back to Cartesian velocity coordinates by use of Eq. (35).

This bearings-only TMA solution, Eq. (46), may be particularly useful at long ranges since the "range collapse" phenomenon can be prevented by a measured or judiciously assumed value for V_R . The bearings-only TMA algorithm minimizes only the cross-range errors. This can cause large down-range errors since they are not minimized. By allowing V_R to be set at an independently measured value, or at some value that is a priori known to be reasonable, a more accurate solution will usually result at the longer ranges.

When it is assumed that $V_R = 0$, this TMA algorithm reduces to a least-squares linear regression formulation of the Ekelund bearings-only range and cross-range velocity algorithm. Note that when $V_R = 0$, Eq. (46) reduces to Eq. (21), except that the velocity components \dot{U} and \dot{W} are changed to $-s_k V_{CR}$ and $c_k V_{CR}$ respectively. Then using Eq. (37), $V_{CR} = -s_k \dot{U} + c_k \dot{W}$, since $\dot{U} = -s_k V_{CR}$ and $\dot{W} = c_k V_{CR}$.

CHAPTER 3

SIMULATION ANALYSIS OF THE TMA ALGORITHMS

A simulation analysis was conducted using the TMA algorithms described by Eq. (9), the $(2, 2 \times 2; R - B)$ algorithm; Eq. (18), the $(4 \times 4; R - B)$ algorithm; Eq. (21), the $(B - 0)$ algorithm; and Eq. (24), the $[K(R - B) + (B - 0)]$ algorithm. The objectives of this simulation analysis were to:

- compare the TMA solution accuracies of these four algorithms,
- confirm the validity of Eq. (27), which derives the weighting coefficient, K , that minimizes the variances of the $[K(R - B) + (B - 0)]$ TMA solution errors,
- confirm the validity of Eqs. (16) and (33) which give the weighting coefficients α_i , that minimize the TMA solution variances of the $(2, 2 \times 2, R - B)$ and the $[K(R - B) + (B - 0)]$ algorithms, respectively, and
- test the effect of a target maneuver upon the TMA solution accuracies of these four algorithms.

A number of statistical methods could have been used to perform the statistical analysis of the TMA algorithms. The method that was used was selected because it provides a zero-mean, symmetrical error distribution of the target data (i.e., the target bearing and the delta-tau, $\Delta\tau$, used to calculate target range) as a function of time. In this method, the error for each bearing is either plus or minus a fixed value, and the error for each delta-tau is also either plus or minus a fixed value, independent of the bearing error. A total of either four or six sets of data as a function of time was used. A TMA solution was obtained for each and every possible permutation of bearing and delta-tau errors which gave a total of $2^4 \cdot 2^4 = 256$

solutions for the four sets of data and $2^6 \cdot 2^6 = 4096$ solutions for the six sets of data. Each TMA solution, consisting of the X and Y components of both initial target position and velocity, was used to solve for target range, down-range velocity and cross-range velocity for the end of the solution time. The mean and standard deviation of these 256 or 4096 solutions were then calculated and used to specify the standard deviation and bias of the target range, and of the down-range and cross-range components of target velocity at the end of the solution time.

3.1 TMA ALGORITHMS ACCURACY COMPARISONS

The first simulation analysis was used to compare the accuracies of the (2, 2 x 2; R - B) and the (4 x 4, R - B) algorithms for a selected group of typical TMA run geometries as shown in Figure 3-1. As expected, the (2, 2 x 2; R - B) algorithm invariably gave more accurate TMA solutions than the (4 x 4, R - B) algorithm, which had horrendous cross-range velocity and TMA bearing errors, especially at long ranges. The cause of these large cross-range target position and velocity errors can be inferred from an inspection of Eq. (18), the residual variance of the (4 x 4, R - B) TMA algorithm. Note that the only errors in this equation are the down-range errors. The linear regression algorithm minimizes these errors, but it does so at the expense of the cross-range errors, which can increase virtually without bounds. For example, the cross-range target velocity error can be as much as hundreds of knots for reasonable values of range, range measurement error and bearing measurement error. In addition to having cross-range errors that were hundreds of times larger those of the (2, 2 x 2; R - B) algorithm, the (4 x 4, R - B) algorithm also had consistently larger range and down-range velocity

TARGET RUN GEOMETRIES

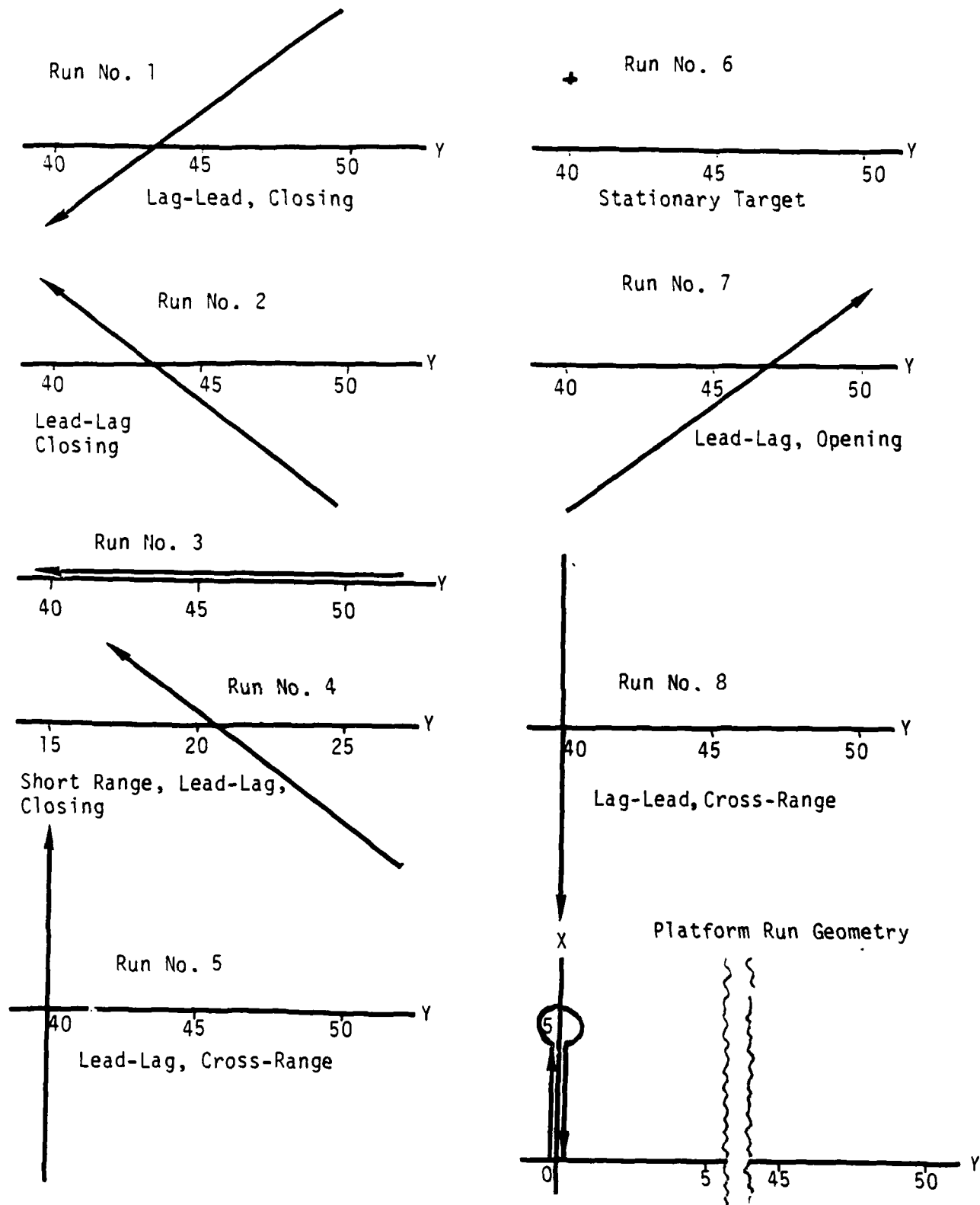


Figure 3-1. Typical Run Geometries Used For TMA Algorithm Comparisons.

errors. This results from the fact that the (4 x 4, R - B) algorithm must simultaneously solve for four unknowns, whereas the (2, 2 x 2; R - B) algorithm, which consists of two sets of equations, must simultaneously solve for only two unknowns. This analysis eliminated the (4 x 4, R - B) algorithm as a candidate for TMA.

3.2 WEIGHTING COEFFICIENT, K_{OPT}

Next, the TMA solution accuracy, as a function of the weighting factor constant, K , was obtained for the $[K(R - B) + (B - 0)]$ algorithm, Eq. (24), for values of K between 0 and 1 inclusive. Note that when $K = 0$, this algorithm becomes the (B - 0) algorithm, Eq. (21), and when $K = 1$, it becomes the (2, 2 x 2, R - B) algorithm, Eq. (9). The value of K which gives the minimum TMA solution error is K_{OPT} as given by Eq. (27). The typical TMA run geometries shown in Figure 3-1 were used to determine the TMA solution errors as a function of K . The results showed that all of the TMA solution errors were at, or very near, their minimum values for $K = K_{OPT}$. They also showed that for values of K between about $0.4 K_{OPT}$ and $2.5 K_{OPT}$, the TMA solution errors were very near their minimum values. Figure 3-2 shows $\sigma(R)$ as a function of K . Figure 3-3 shows $\sigma(R)$, $\sigma(V_R)$ and $\sigma(V_{CR})$ as a function of K for the three most significant values of K : $K = 0$, the (B - 0) TMA algorithm; $K = K_{OPT}$, the $[K_{OPT}(R - B) + (B - 0)]$ TMA algorithm; and $K = 1$, the (2, 2 x 2; R - B) TMA algorithm. The TMA solution errors $\sigma(R)$, $\sigma(V_R)$ and $\sigma(V_{CR})$ are the standard deviation errors of the TMA solutions for R , V_R and V_{CR} , respectively, at the end of the solution time interval (i.e., at the end of the second leg of platform motion). Note that the (B - 0) TMA errors, ($K = 0$), are less than the (2, 2 x 2; R - B) TMA errors, ($K = 1$), for

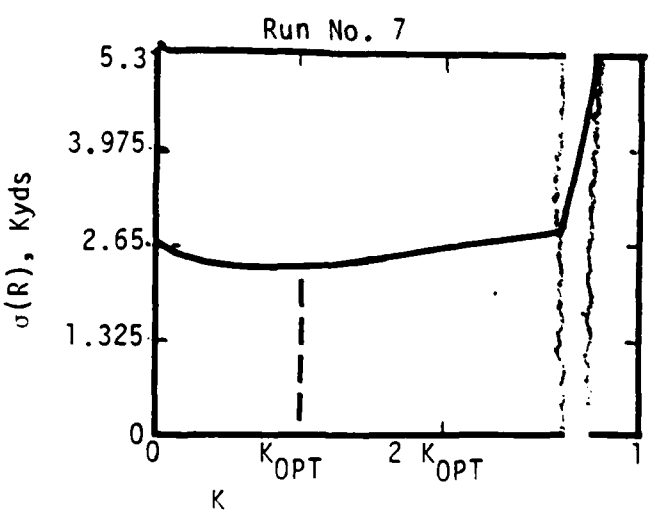
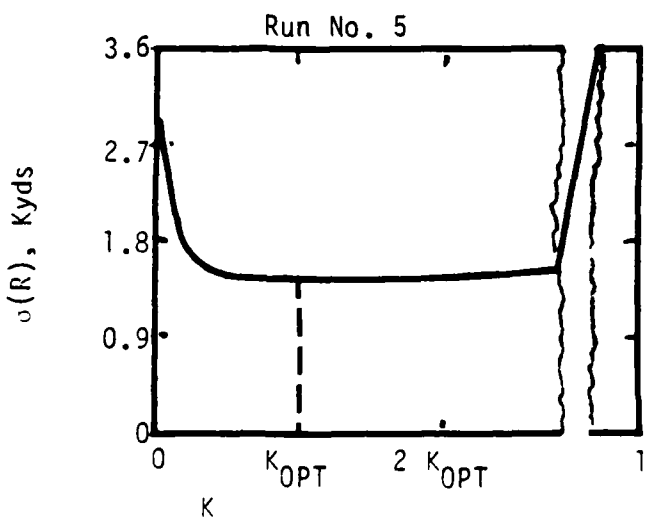
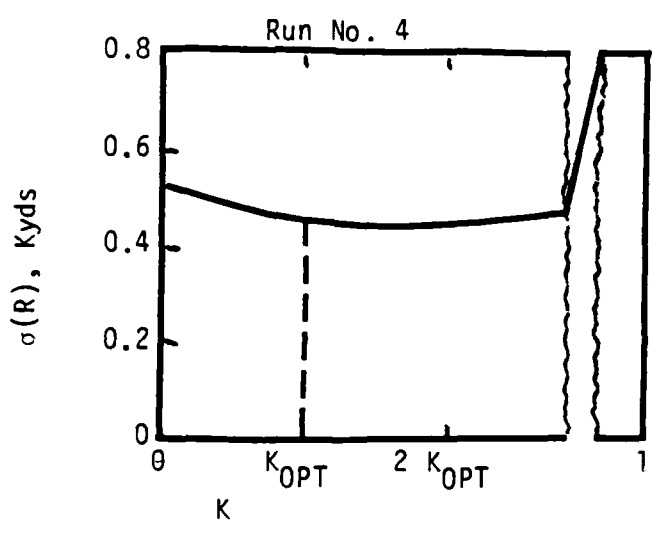
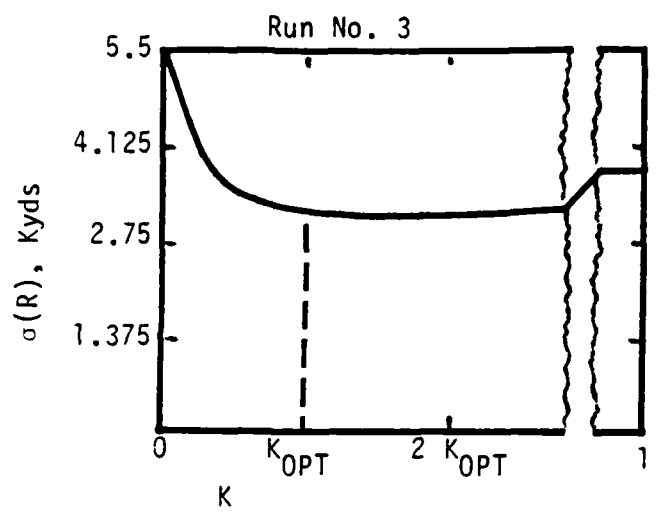
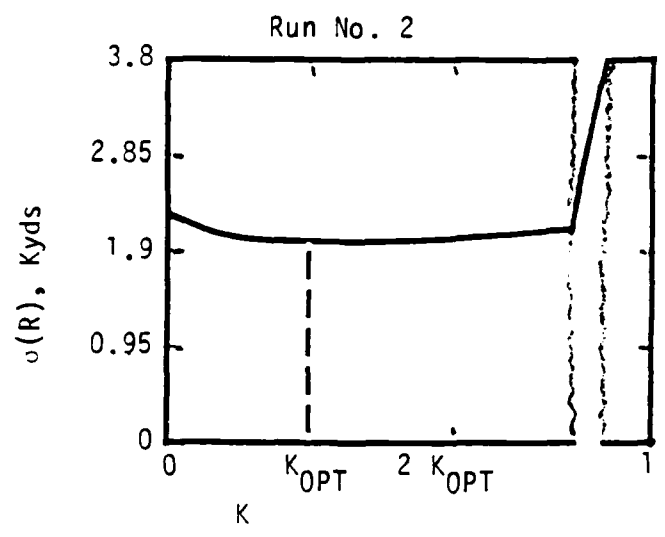
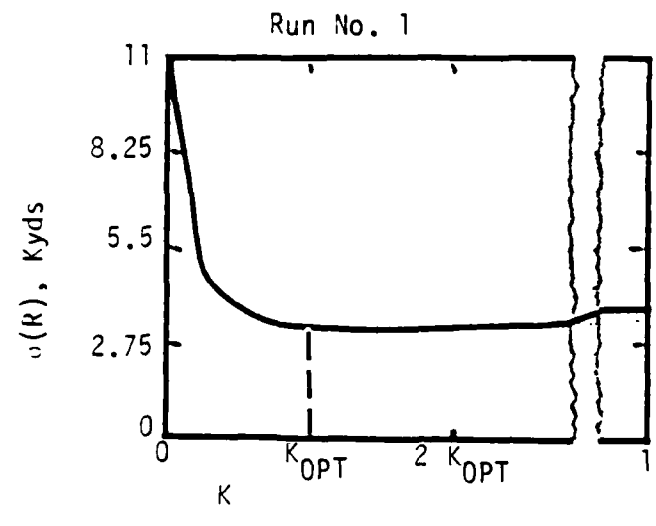


Figure 3-2. $\sigma(R)$ Versus K.

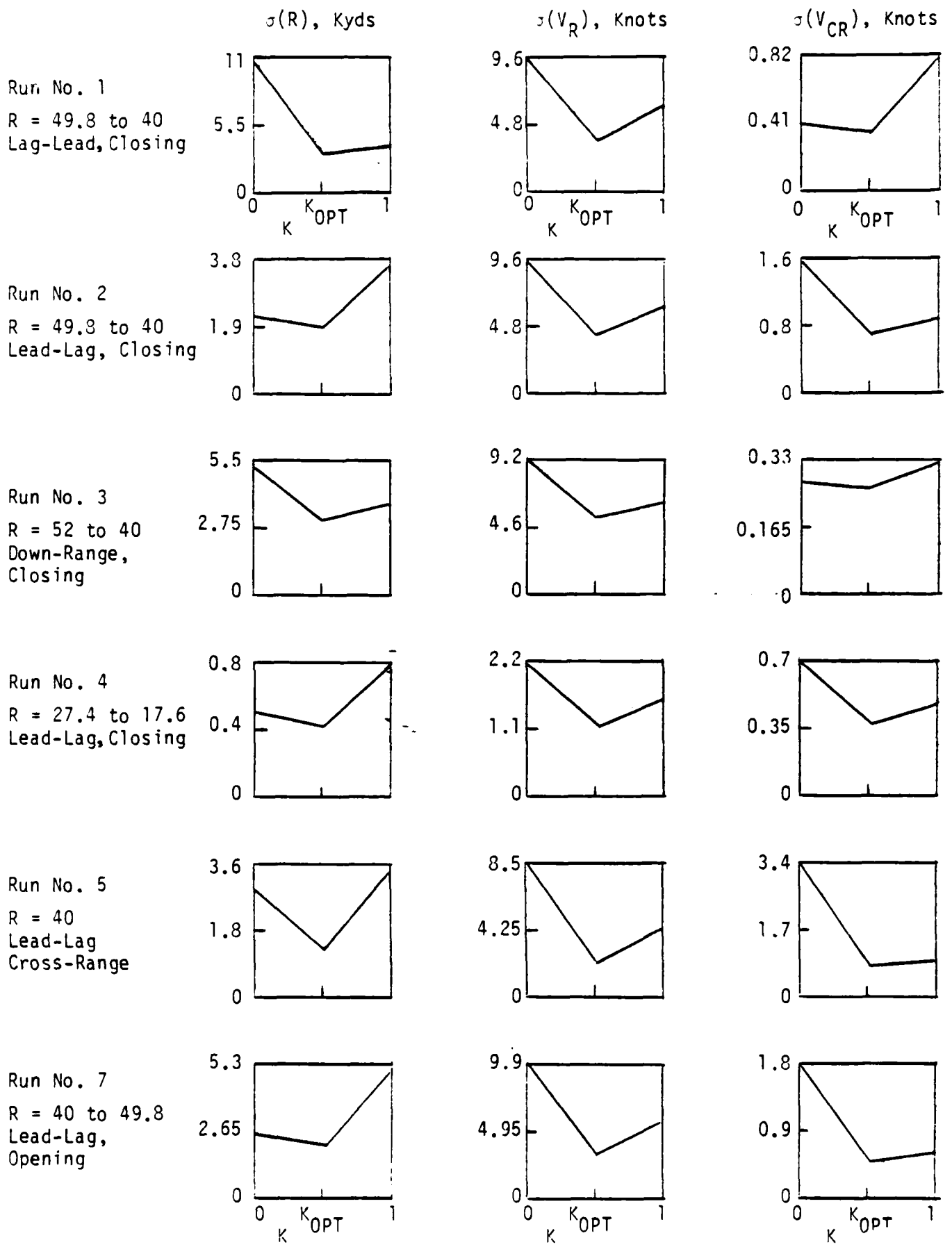


Figure 3-3. $\sigma(R)$, $\sigma(V_R)$ and $\sigma(V_{CR})$ Versus K.

some of the runs and greater for the other runs, but the $[K_{OPT}(R - B) + (B - 0)]$ TMA errors ($K = K_{OPT}$) are less than either for all of the runs.

It is interesting to compare in Figure 3-2 the $\sigma(R)$ versus K curves of runs Nos. 1 and 2. In run No. 1, the platform conducts lag-lead legs of motion and in run No. 2 it conducts lead-lag legs of motion, against a target moving with the same cross-range and down-range velocity components. The $(B - 0)$ TMA algorithm, ($K = 0$), gives a $\sigma(R)$ of 11 kyds for run No. 1 and a $\sigma(R)$ of only 2.35 kyds for run No. 2. This large percentage difference, (468 percent), in the $\sigma(R)$ of the lag-lead versus the lead-lag platform runs for bearings-only TMA was initially described in a previous technical report.¹ The $(2, 2 \times 2, R - B)$ TMA algorithm gives a $\sigma(R)$ of 3.8 kyds for both runs No. 1 and No. 2, thus indicating that this algorithm gives the same TMA accuracy, independent of whether the platform motion is lag-lead or lead-lag. However, the most accurate TMA solution is obtained by using the $[(K_{OPT}(R - B) + (B - 0))]$ algorithm and conducting lead-lag legs of platform motion, as in run No. 2. This gives a $\sigma(R)$ of 2.0 kyds. If the lag-lead legs of platform motion, as in run No. 1, were conducted using this algorithm, $\sigma(R)$ would have been 3.5 kyds, which is about 75 percent greater than for lead-lag legs. Therefore, even though this percentage difference is considerably smaller than that for the $(B - 0)$ algorithm, it is still large enough to justify using lead-lag legs rather than lag-lead legs of two-leg platform motion. Appendix B shows why the lead-lag platform motion tactic gives a more accurate TMA range solution than the lag-lead platform motion tactic.

¹Ibid.

3.3 GEOMETRIC WEIGHTING COEFFICIENT, α_g

The weighting coefficient, α , for weighting each linear equation relative to the others, in the set of equations which comprises the TMA algorithm, is the product of two different weighting factors, the signal-to-noise weighting factor, $\alpha_{S/N}$, Eq. (15), and the geometric weighting factor, α_g , Eq. (33), which gives the optimum weighting coefficient, α , for the $[K_{OPT} (R - B) + (B - 0)]$ TMA algorithm, shows a geometric weighting factor of

$$\left(\frac{\sin \theta}{R}\right)^2.$$

The optimum geometric weighting factor for the $(2, 2 \times 2; R - B)$ TMA algorithm is shown in Eq. (16) to be

$$\left(\frac{\sin \theta}{R}\right)^4,$$

or the square of that for the $[K(R - B) + (B - 0)]$ algorithm.

The five run geometries shown in Figure 3-4 were simulation analyzed in order to determine the validity of these geometric weighting factors. Six sets of data were used to obtain each solution, which gave a total of 4,096 solutions per run that were used to obtain the standard deviation and bias of the TMA range solution.

The range bias error is due to the non-linearity of the range error as a function of bearing error. If the bearing error is assumed to be a zero-mean random error with a symmetrical distribution, a reasonable assumption, the range error distribution is skewed (i.e., it is both biased and non-symmetrical). A simple example will show this non-linearity. Let the range to a stationary target be determined by measuring the target bearing from two different locations, A and B, that are separated by a distance L which is

¹Ibid.

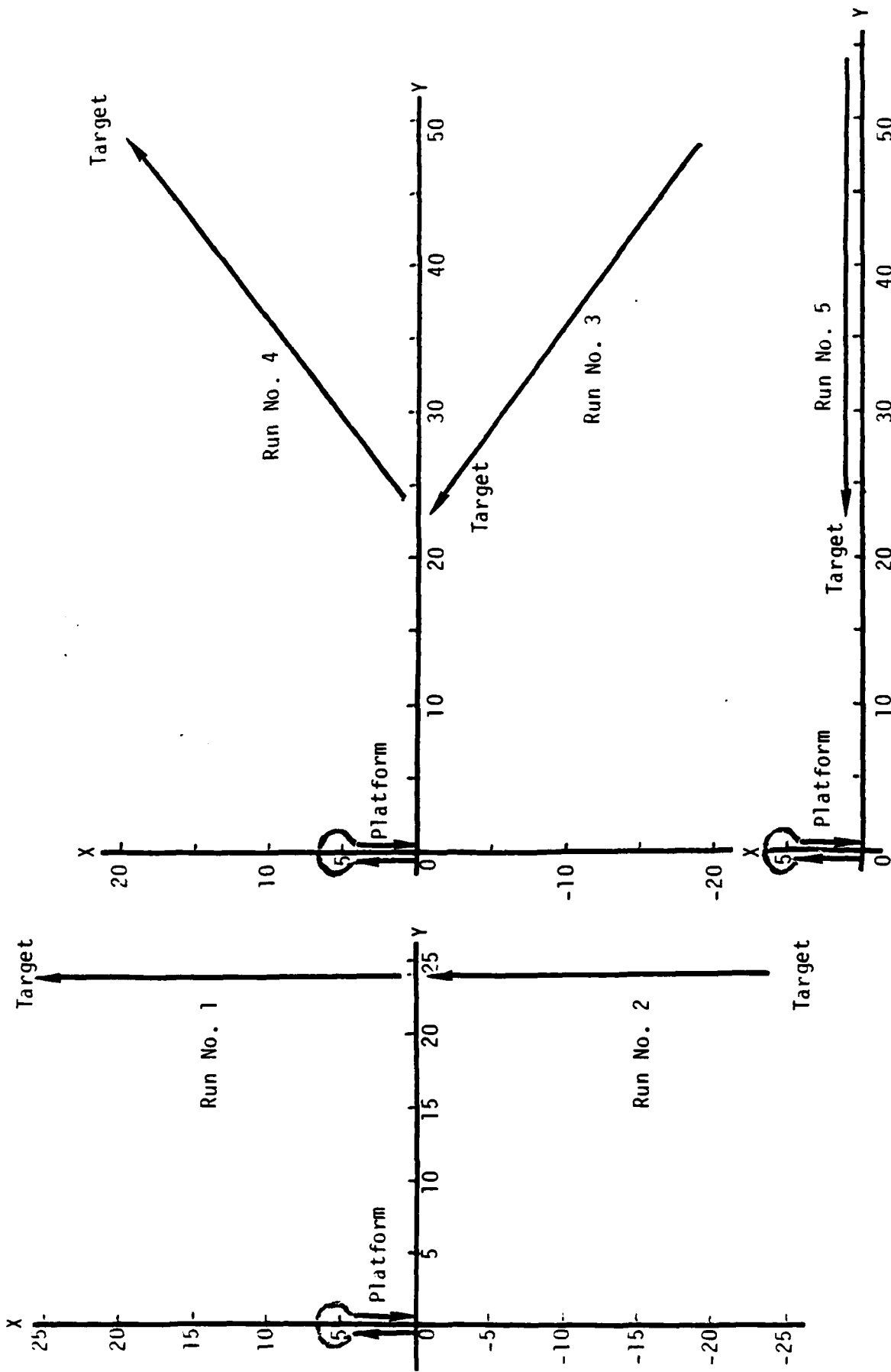


Figure 3-4. Run Geometries Used to Analyze the Geometric Weighting Factor, "g".

assumed to be small compared to the range. For this case the actual range is

$$\hat{R} \approx \frac{L \sin \frac{1}{2} (\theta_A + \theta_B)}{\theta_B - \theta_A} = \frac{L \sin \theta}{\Delta \theta} \quad (46)$$

If it is assumed that the error in $\Delta \theta$ is plus or minus $E(\Delta \theta)$, the simplest possible symmetric distribution, then calculated ranges are the following:

$$R_+ = \frac{L \sin \theta}{\Delta \theta + E(\Delta \theta)} = \frac{\hat{R}}{1 + \frac{E(\Delta \theta)}{\Delta \theta}} = \frac{\hat{R}}{1 + e}$$

$$R_- = \frac{L \sin \theta}{\Delta \theta - E(\Delta \theta)} = \frac{\hat{R}}{1 - \frac{E(\Delta \theta)}{\Delta \theta}} = \frac{\hat{R}}{1 - e} \quad (47)$$

where

$$e = \frac{E(\Delta \theta)}{\Delta \theta}$$

The range bias is;

$$\text{BIAS}(R) = \frac{e^2 \hat{R}}{1 - e^2} \quad (48)$$

Note that the bias is positive if e^2 is less than one, negative if e^2 is greater than one, and approaches plus or minus infinity as e^2 increases to one or decreases to one, respectively.

The derivations of the optimum geometric weighting factors were based upon the assumption that the TMA solution errors were linear. This is a valid assumption for small range and bearing measurement errors at short ranges, but it is not necessarily valid for the moderate range and bearing errors and the longer ranges that are often encountered in actual target engagements.

Therefore, in order to determine the optimum geometric weighting factor under the more realistic conditions where range bias may be a significant fraction of the total TMA range error, the simulation analysis assumed bearing errors of plus or minus 0.5 degrees and range errors (due to a delta-tau error in the WAA of plus or minus 2.5 microseconds) which resulted in biased range inputs

to the TMA algorithms. The results of this simulation analysis for the (2, 2 x 2; R - B) and the $[K_{OPT}(R - B) + (B - 0)]$ TMA algorithms are given in Figure 3-5, which shows $\sigma(R)$ and $RMS(R)$ versus α_g for the two algorithms and for each of the five run geometries. The $RMS(R)$ is

$$RMS(R) = \left[\sigma^2(R) + BIAS^2(R) \right]^{\frac{1}{2}} \quad (49)$$

The optimum geometric weighting factor for the $[K_{OPT}(R - B) + (B - 0)]$ TMA algorithm using the $RMS(R)$ curves varies somewhat for the five runs, but

$$\left(\frac{\sin \theta}{R} \right)^2$$

is a reasonable value overall, just as predicted by Eq. (33). The optimum geometric weighting factor for the (2, 2 x 2; R - B) TMA algorithm probably lies closer to

$$\left(\frac{\sin \theta}{R} \right)^3$$

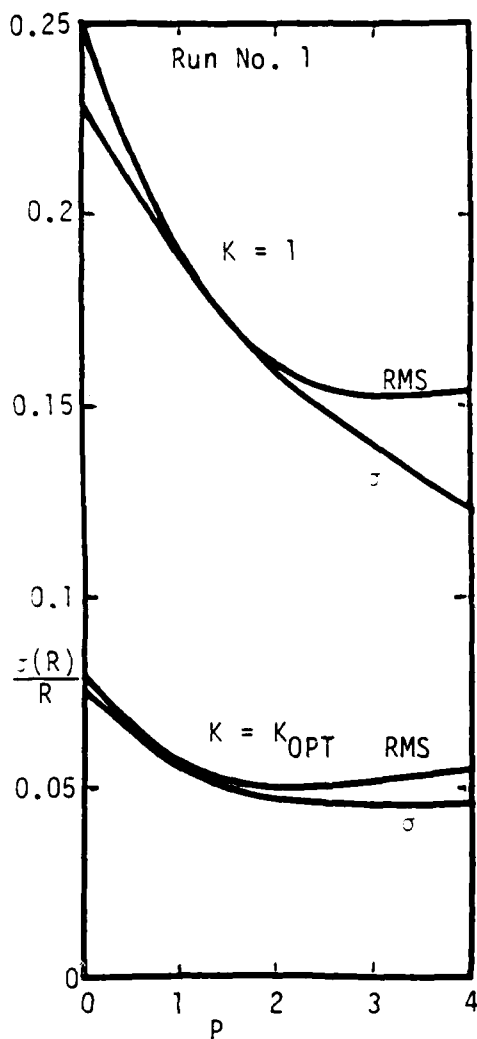
than to

$$\left(\frac{\sin \theta}{R} \right)^4$$

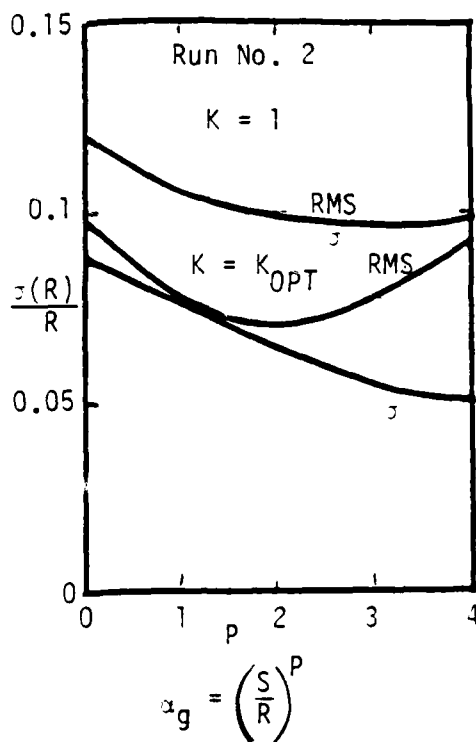
as was predicted by Eq. (16). However, the difference is so small that Eq. (16) may be used as the optimum weighting coefficient.

3.4 MANEUVERING TARGET INDUCED TMA ERRORS

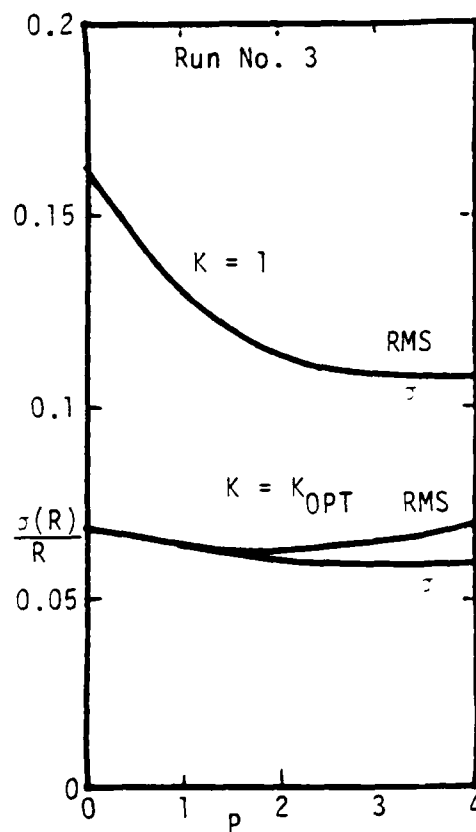
Maneuvering targets pose a special problem for TMA algorithms since they are all based upon Eqs. (1) and (2), which are for a constant velocity target motion. In order to directly compare the accuracies of the (B - 0), $[K_{OPT}(R - B) + (B - 0)]$ and (2, 2 x 2; R - B) TMA algorithms, a simulation analysis was performed using the nine run geometries shown in Figure 3-6, eight of which contain a target maneuver. Note that part of each of the target



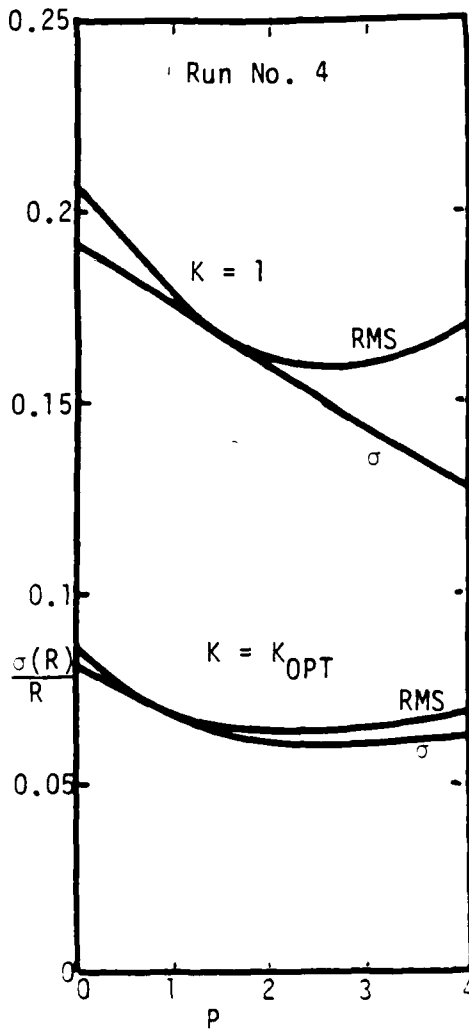
$$\alpha_g = \left(\frac{S}{R}\right)^p$$



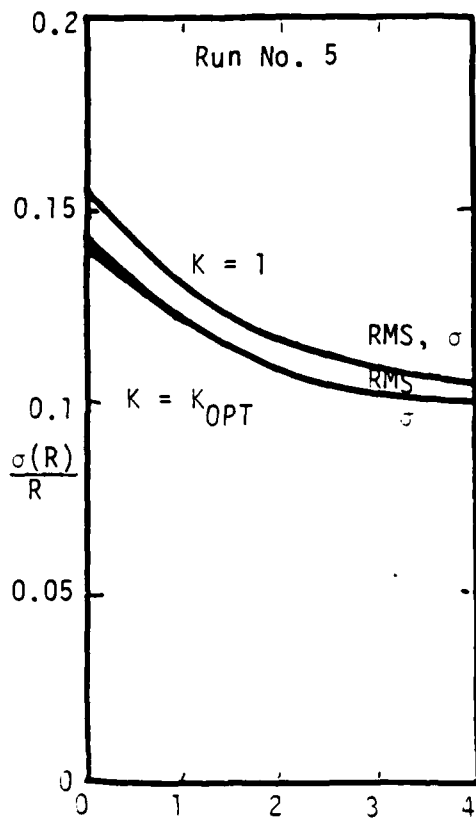
$$\alpha_g = \left(\frac{S}{R}\right)^p$$



$$\alpha_g = \left(\frac{S}{R}\right)^p$$



$$\alpha_g = \left(\frac{S}{R}\right)^p$$



$$\alpha_g = \left(\frac{S}{R}\right)^p$$

Figure 3-5. $\sigma(R)$ and $RMS(R)$ Versus Geometric Weighting Factor, α_g .

TARGET RUN GEOMETRIES

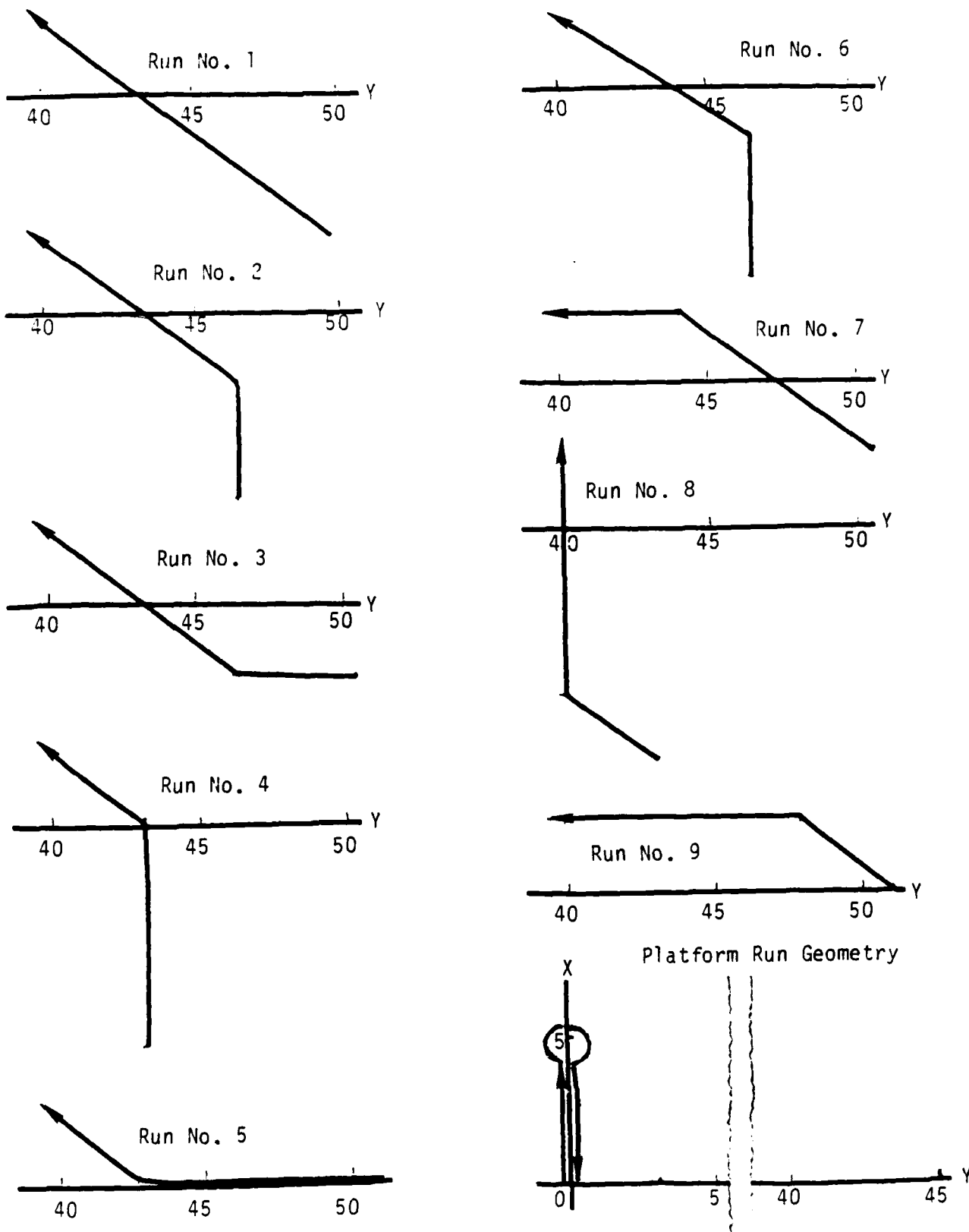


Figure 3-6. Maneuvering Target Run Geometries Used For TMA Error Analysis.

maneuver runs is the same as the constant velocity target run. Four sets of data (at the beginning and end of each leg of platform motion) were used to obtain each solution, which gave a total of 256 solutions per run that were then used to obtain the standard deviation and bias of the TMA solution for range, down-range target velocity and cross-range target velocity. This was done for each run and for each of the three TMA algorithms. The analysis results are listed in Table 3-1. The absolute mean values for the eight maneuvering target runs are given in Figure 3-7 as a function of K for $K = 0$, the $(B - 0)$ TMA algorithm; $K = K_{OPT}$, the $[K_{OPT} (R - B) + (B - 0)]$ TMA algorithm; and $K = 1$, the $(2, 2 \times 2, R - B)$ TMA algorithm. The dashed curves in the $\sigma(R)$, $BIAS(R)$ and $RMS(R)$ versus K figures are for run No. 1, which is the non-maneuvering target run. Note that the range errors for $K = 1$, the $(2, 2 \times 2; R - B)$ algorithm, are not significantly greater for the maneuvering target runs than for run No. 1. Conversely, the $RMS(R)$ error for $K = 0$, the $(B - 0)$ algorithm, is 2.7 times as large for the maneuvering target runs, due primarily to the large $BIAS(R)$ error.

While the eight maneuvering target runs that were analyzed represent only a small sample out of the infinite set of possible target maneuvers, it nevertheless bridges the gap between non-maneuvering target runs and those maneuvering target runs which can be detected by a maneuver detection algorithm. The analysis shows that whenever range measurement data is available, the $(2, 2 \times 2; R - B)$ TMA algorithm gives the most accurate range solution and a reasonably accurate target velocity solution for a maneuvering target. The $(B - 0)$ TMA algorithm solution for a maneuvering target tends to diverge, which causes unacceptably large bias errors. The $[K_{OPT} (R - B) + (B - 0)]$ TMA solution, as might be expected, has bias errors that are

Table 3-1. Maneuvering Target Results

(a) $K = 0$, the $(B - 0)$ TMA Algorithm

Run No.	$\frac{\sigma(R)}{R}$	$\frac{\text{Bias}(R)}{R}$	$\frac{\sigma(V_R)}{V_P}$	$\frac{B(V_R)}{V_P}$	$\frac{\sigma(V_{CR})}{V_P}$	$\frac{B(V_{CR})}{V_P}$
1	0.1065	0.0084	1.234	0.266	0.213	0.038
2	0.1865	0.2579	2.496	0.0417	0.590	-0.305
3	0.092	-0.1403	0.697	1.185	0.074	0.385
4	0.1225	0.2176	1.17	2.122	0.356	-0.018
5	0.0939	-0.3518	0.908	-0.964	0.077	0.408
6	0.0876	-0.1007	1.171	0.445	0.271	0.277
7	0.2214	0.5823	1.717	3.069	0.189	-0.281
8	0.0533	-0.196	0.529	0.784	0.321	0.545
9	0.2645	0.1909	2.983	-2.685	0.210	-0.396
Mean	0.140	0.255	1.459	1.412	0.237	0.327
σ	0.070	0.143	0.820	1.02	0.161	0.143

(b) $K = K_{OPT}$, the $[K_{OPT}(R - B) + (B - 0)]$ TMA Algorithm

Run No.	$\frac{\sigma(R)}{R}$	$\frac{\text{Bias}(R)}{R}$	$\frac{\sigma(V_R)}{V_P}$	$\frac{B(V_R)}{V_P}$	$\frac{\sigma(V_{CR})}{V_P}$	$\frac{B(V_{CR})}{V_P}$
1	0.0901	0.0061				
2	0.0975	0.167	0.681	0.644	0.131	-0.118
3	0.0851	-0.134	0.681	0.067	0.083	0.232
4	0.0891	0.200	0.542	1.398	0.131	-0.200
5	0.0924	-0.256	0.772	-0.995	0.070	0.392
6	0.0772	-0.066	0.640	-0.438	0.134	0.256
7	0.1295	0.307	0.831	1.355	0.087	-0.386
8	0.582	-0.143	0.467	-0.355	0.121	0.182
9	0.1354	0.151	0.961	0.076	0.069	-0.193
Mean	0.0956	0.178	0.698	0.666	0.103	0.245
σ	0.0241	0.070	0.148	0.497	0.027	0.091

Table 3-1. Maneuvering Target Results (Continued)

(c) $K = 1$, the (2, 2 x 2, R + B) TMA Algorithm

Run No.	$\frac{\sigma(R)}{R}$	$\frac{\text{Bias}(R)}{R}$	$\frac{\sigma(V_R)}{V_P}$	$\frac{B(V_R)}{V_P}$	$\frac{\sigma(V_{CR})}{V_P}$	$\frac{B(V_{CR})}{V_P}$
1	0.160	0.040	1.038	-0.140	0.154	-0.046
2	0.107	0.194	0.753	0.734	0.137	-0.117
3	0.160	0.036	1.052	-0.214	0.126	0.132
4	0.156	0.071	0.896	0.535	0.177	-0.301
5	0.161	0.032	1.075	-0.328	0.093	-0.400
6	0.167	0.100	0.987	1.039	0.175	0.306
7	0.162	0.049	1.059	0.023	0.114	-0.453
8	0.148	0.025	0.870	-0.289	0.181	0.050
9	0.163	0.045	1.082	-0.093	0.081	-0.186
Mean	0.153	0.069	0.972	0.407	0.136	0.243
σ	0.018	0.052	0.112	0.321	0.037	0.135

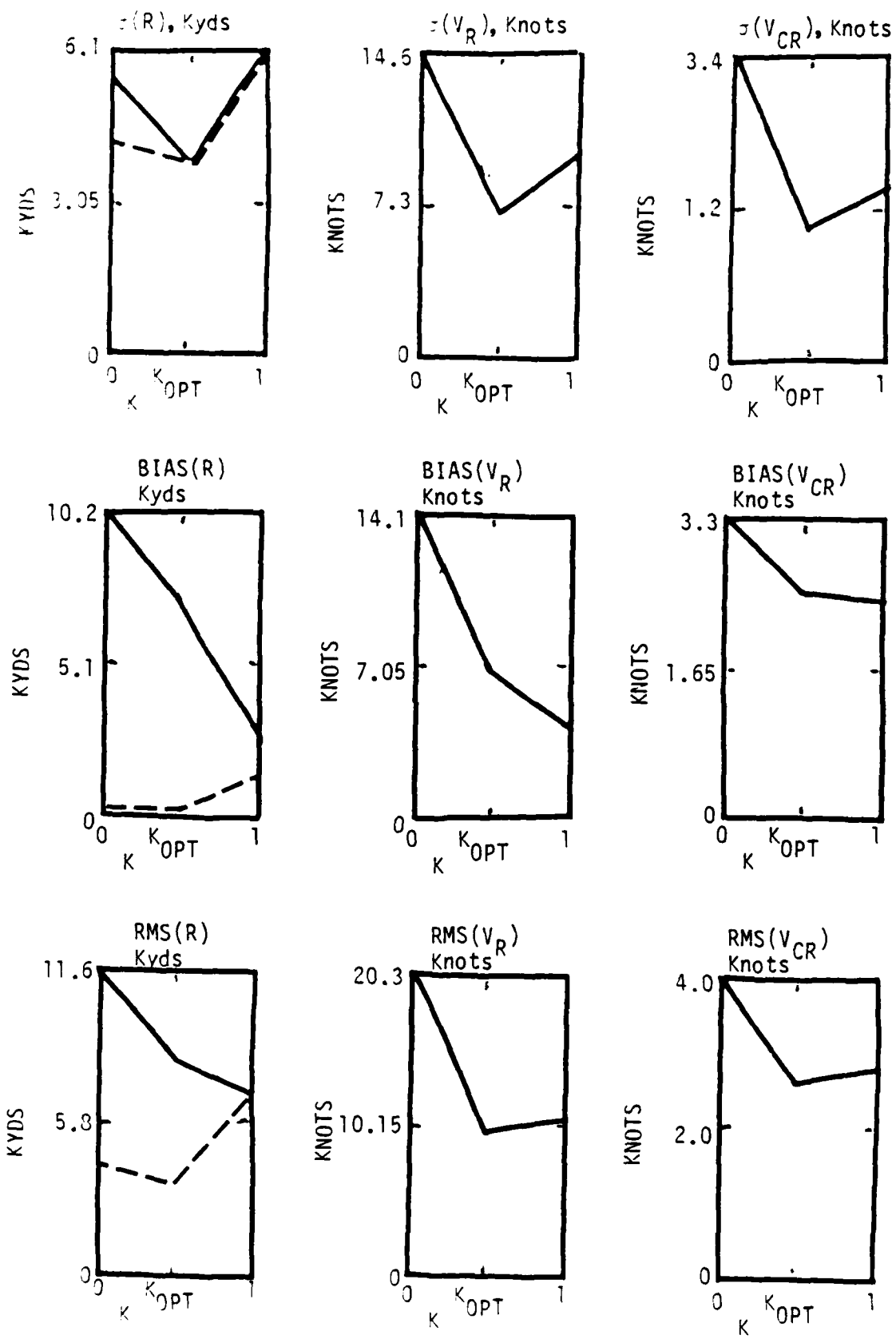


Figure 3-7. TMA Errors Versus K for Maneuvering Target Runs.

intermediate between the other two algorithms, but the standard deviation errors are significantly less than for either of the others. Therefore, the root-mean-square errors are not unreasonably higher than those of the (2, 2 x 2; R - B) algorithm.

The computer programming and the computations used for the simulation analyses of the TMA algorithms were provided by Mr. Juan Arvelo of the Naval Surface Weapons Center, Code U21. His significant contribution to this work is gratefully acknowledged.

CHAPTER 4

CONCLUSIONS AND RECOMMENDATIONS

This report has shown that the accuracies of TMA solutions are significantly improved by the proper addition of range measurement data to the least-squares linear-regression TMA algorithms, all of which belong to the non-recursive (or batch) type of linear prediction filter. Even though range measurement data can also improve the accuracies of Kalman filter TMA algorithms (which are a recursive type of linear prediction filter), the non-recursive type of filter is inherently more stable (i.e., less prone to give a diverged solution) and more accurate. In fact, the recursive filter is simply a constant-velocity-target tracker, given that the initial target position and/or velocity are either known or assumed with a sufficient degree of accuracy. Conversely, the non-recursive filter actually solves for the constant-velocity target position as a function of time (i.e., the target position at a given time and the target velocity). Therefore, it is recommended that all Kalman filter TMA algorithms for use in underwater fire control systems be replaced by the appropriate least-squares linear-regression TMA algorithms.

The most accurate TMA algorithm for using both range and bearing data was shown to be the $[K_{OPT}(R - B) + (B - O)]$ TMA algorithm. Practical methods of determining K_{OPT} were derived and shown to be valid for a variety of typical target run geometries. It is recommended that this algorithm be implemented into the fire control systems of ships and submarines that have accurate range-measuring sonar systems.

Real targets will most likely maneuver at frequent pseudo-random intervals when in potentially hostile areas or when alerted to the presence of a threat target. The $(2, 2 \times 2; R - B)$ TMA algorithm was shown to be the least affected by target maneuvers. Therefore, it is recommended that this algorithm also be implemented into the above fire control systems.

A $(B - 0)$ TMA algorithm was initially implemented in the Mk 113 Fire Control System where it was called CHURN. It has been supplanted by an operator-computer interactive system called MATE which is inherently superior to the basic $(B - 0)$ TMA algorithm since it contains a method for detecting target maneuvers and for casting out bad data. It is highly recommended that all the TMA algorithms be provided with maneuver detection and bad data removal algorithms. MATE calculates from the TMA solution what each bearing would have been at the time of each measurement and subtracts it from the measured bearing to give a plot of bearing deviation versus time, which is displayed on an output screen for the operator to view. Deviations which increase or decrease linearly with time indicate a target maneuver. A few scattered deviations that are significantly larger than the others may be cast out as representing bad data and a new TMA solution can be calculated with these data deleted. An algorithm can be developed to automatically cast out bad data points and relieve the operator from this task. It is also recommended that the $(B - 0)$ TMA algorithm be implemented for use whenever range data is unavailable. This is simply done by setting $K = 0$ in the $[K(R - B) + (B - 0)]$ TMA algorithm.

With only slight modifications both the $(2, 2 \times 2; R - B)$ and the $(B - 0)$ TMA algorithms can be used whenever the value of V_p , the down-range component of target velocity, is either known or assumed to be known as described in the report. The usefulness of these algorithms has not been established.

However, Ekelund ranging is extensively used in field tests and it provides range solutions that are often more accurate than those from the TMA algorithms. Since the (B - 0) TMA algorithm for an assumed value of V_R , given by Eq. (46), is the least-squares linear-regression formulation of the Ekelund algorithm, it should provide even more accurate range and cross-range velocity solutions. A similar argument holds for the (2, 2 x 2; R - B) TMA algorithm for an assumed value of V_R , as given by Eq. (36). It is, therefore, recommended that these two algorithms be field tested to determine whether or not they should be implemented into the appropriate fire control systems.

The optimum weighting coefficient, α_{OPT} , for weighting each linear equation relative to the others was derived for each algorithm and then tested by simulation analysis for which the input data errors were not unreasonably large, but still large enough to give biased range measurements. These biases affected the optimum geometric weighting factors somewhat, but not enough to justify changing them. It is recommended that the appropriate α_{OPT} be used in each of the TMA algorithms. It may also be desirable to provide the option of including a time dependent factor to α_{OPT} in order to reduce the magnitudes of the TMA solution bias errors that are caused by a target maneuver. An empirically determined time-dependent weighting factor is the following:

$$(\alpha_t)_i = 1 + \left(\frac{v_p t}{5 R} \right)_i^2 \quad (50)$$

where

v_p = platform speed in knots

t_i = time after t_0 in minutes

R_i = averaged measured range at time t_i in kiloyards

This weighting factor should decrease the TMA solution bias errors for maneuvering targets, but it will slightly increase the TMA solution standard deviation error for non-maneuvering targets.

CHAPTER 5
NOMENCLATURE

(U, W) = initial target position (unknown)

(\dot{U}, \dot{W}) = target velocity (unknown)

$(U_i, W_i) = (U + t_i \dot{U}, W + t_i \dot{W})$

$t = t_i$ = time since initial time, ($t_1 = 0$)

$(\hat{X}, \hat{Y}) = (\hat{X}_i, \hat{Y}_i)$ = platform position at time t_i

$(X, Y) = (X_i, Y_i)$ = measured platform position at time t_i

$E(X) = X - \hat{X}$ = error in measured value of X

$E(Y) = Y - \hat{Y}$ = error in measured value of Y

$\hat{R} = \hat{R}_i$ = target range (from platform) at time t_i

$R = R_i$ = measured target range at time t_i

$E(R) = R - \hat{R}$ = error in measured range

$\hat{B} = \hat{B}_i$ = true bearing to target at time t_i

$B = B_i$ = measured true bearing to target at time t_i

$E(B) = B - \hat{B}$ = error in measured true bearing

$\hat{s} = \sin \hat{B} = \sin [B - E(B)] \approx \sin B - (\cos B) E(B) \approx S - cE(B)$

$s = \sin B$

$\hat{c} = \cos \hat{B} = \cos [B - E(B)] \approx \cos B + (\sin B) E(B) = c + s E(B)$

$c = \cos B$

$E(s) \approx (\cos B) E(B) = c E(B)$ = error in $\sin B$ due to $E(B)$ (a first order approximation)

$E(c) \approx -(\sin B) E(B) = -s E(B)$ = error in $\cos B$ due to $E(B)$ (a first order approximation)

$\alpha = \alpha_j$ = a weighting coefficient for the i th equation in the set of n equations

K = a weighting coefficient for the range-bearing TMA solution relative to the bearings-only TMA solution

$V_{CR} = V_{CR}(t = t_k)$ = cross-range component of target velocity at time t_k

$V_R = V_R(t = t_k)$ = down-range component of target velocity at time t_k

$(\dot{R}_{\text{PLATFORM}})_K = (V_p \cos \theta)_K$ = down-range component of platform velocity at time t_k

$\overline{\dot{R}_{\text{PLATFORM}}}$ = mean down-range component of platform velocity from time $t = 0$ to time $t = t_k$

$(\tilde{R})_K$ = TMA range at time t_k

MEDIAN(R) = median value of measured range

$$A_{11} = \sum \alpha c^2$$

$$A_{12} = \sum \alpha t c^2$$

$$A_{13} = \sum \alpha s c$$

$$A_{14} = \sum \alpha t s c$$

$$A_{22} = \sum \alpha t^2 c^2$$

$$A_{24} = \sum \alpha t^2 s c$$

$$A_{33} = \sum \alpha s^2$$

$$A_{34} = \sum \alpha t s^2$$

$$A_{44} = \sum \alpha t^2 s^2$$

$$B_{11} = \sum \alpha$$

$$B_{12} = \sum \alpha t$$

$$B_{12} = \sum \alpha t^2$$

$$F_1 = \sum \alpha (Rc + X)$$

$$F_2 = \sum \alpha t (Rc + X)$$

$$F_3 = \sum \alpha (Rs + Y)$$

$$F_4 = \sum \alpha t (Rs + Y)$$

$$D_1 = \sum \alpha c (R + cX + sY)$$

$$D_2 = \sum \alpha t c (R + cX + sY)$$

$$D_3 = \sum \alpha s (R + cX + sY)$$

$$D_4 = \sum \alpha t s (R + cX + sY)$$

$$E_1 = \sum \alpha s (sX - cY)$$

$$E_2 = \sum \alpha t s (sX - cY)$$

$$E_3 = - \sum \alpha c (sX - cY)$$

$$E_4 = - \sum \alpha t c (sX - cY)$$

APPENDIX A

KOPT For $[K(R - B) + (B - 0)]$ TMA Algorithm Using D/E or Multipath Ranging Data

Figure A-1 shows the geometry for D/E or multipath ranging. The figure shows straightline propagation paths, when in reality these paths may be curved due to temperature and pressure gradients. Therefore, it is assumed that each actual path has been ray-path-curvature corrected to its equivalent straightline path. The target range is

$$R = (D - P) \cot \phi + (D - T) \cot (\phi + 2\alpha) \quad (\text{A-1})$$

where

D = ocean depth at the reflection point

α = ocean bottom down-range slope at the reflection point

= $E(\alpha)$ if α is not known

P = platform depth

ϕ = vertical arrival angle of the broadband radiated target signal

T = target depth

The range error, to a first order approximation is

$$E(R) = [\cot \phi + \cot (\phi + 2\alpha)] E(D) - \cot (\phi + 2\alpha) E(T) \\ - \left[\frac{D - P}{\sin^2 \phi} + \frac{D - T}{\sin^2 (\phi + 2\alpha)} \right] E(\phi) + \frac{2(D - T)}{\sin^2 (\phi + 2\alpha)} E(\alpha) \quad (\text{A-2})$$

If it is assumed that $\alpha \ll \phi$ and $P, T \ll D$

$$E(R) = R \left[\frac{2 E(D) - E(T)}{2D} + \frac{2 E(\alpha) - 2 E(\phi)}{\sin 2\phi} \right]$$

$$\sigma(R) = R \sqrt{\sigma^2(R)_D + \sigma^2(R)_T + \sigma^2(R)_\alpha + \sigma^2(R)_\phi} \quad (\text{A-3})$$

where

$$\sigma(R)_D = \frac{R}{D} \sigma(D)$$

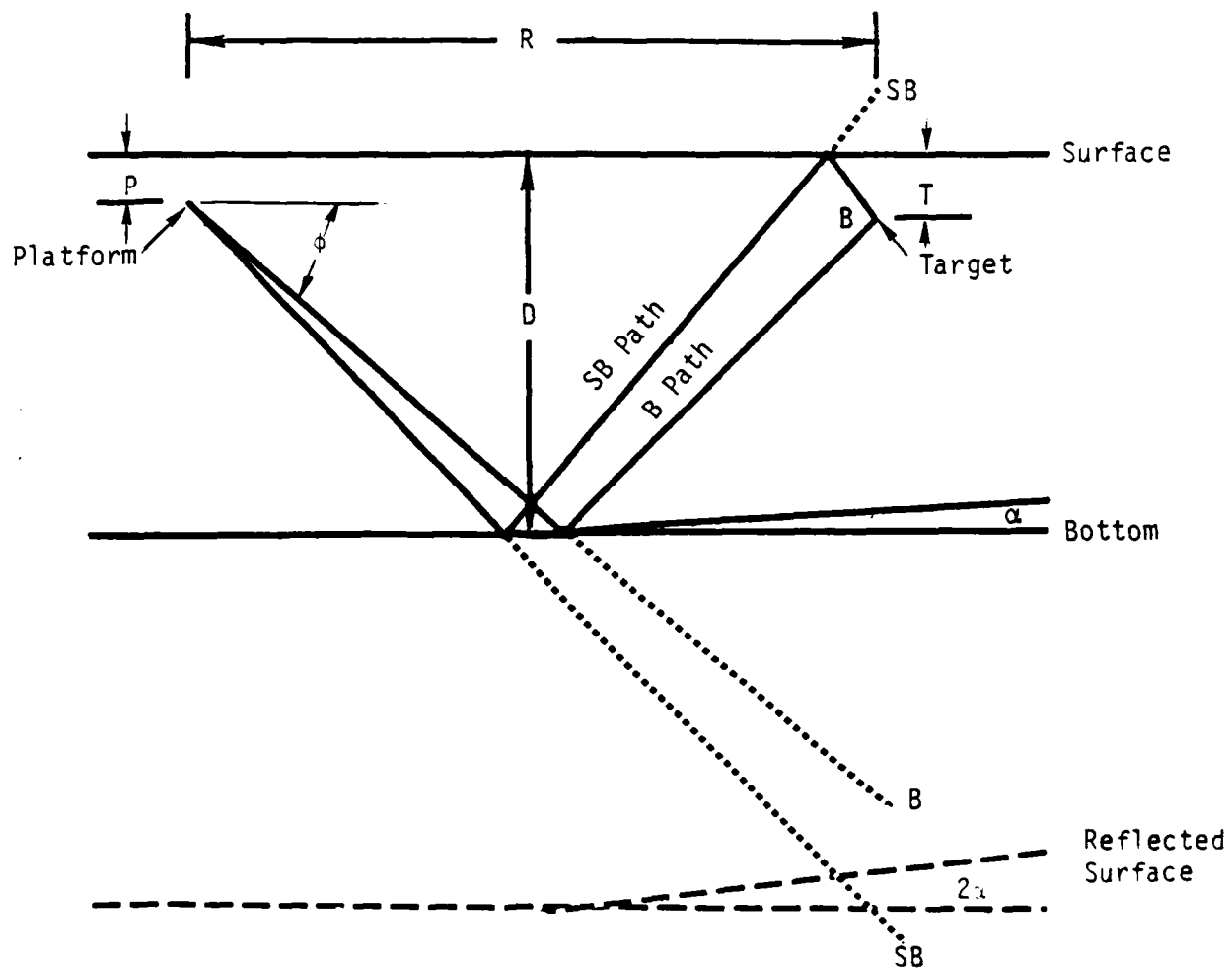


Figure A-1. Geometry for D/E or Multipath Ranging.

$$\sigma(R)_T = \frac{R}{2D} \sigma(T)$$

$$\sigma(R)_\alpha = \frac{2R}{\sin 2\phi} \sigma(\alpha) = \frac{R \sigma(\alpha)}{\sin \phi \cos \phi}$$

$$\sigma(R)_\phi = \frac{2R}{\sin 2\phi} \sigma(\phi) = \frac{R \sigma(\alpha)}{\sin \phi \cos \phi}$$

The value of K which minimizes the $[K(R - B) + (B - 0)]$ TMA solution errors is

$$K_{OPT} = \left[\frac{R \sigma(B)}{\sigma(R)} \right]^2 \quad (A-4)$$

A reasonable example of the errors $\sigma(B)$ and those which comprise $\sigma(R)$ are the following:

Let

$$\sigma(D) = 450' = 0.15 \text{ kyds}$$

$$\sigma(\phi) = 1^\circ = 0.0175 \text{ radians}$$

$$\sigma(\alpha) = 1^\circ$$

$$\sigma(B) = \sigma(\alpha) = 1^\circ \text{ (in bottom-bounce mode)}$$

Substituting these standard deviation errors into Eqs. (A-3) and (A-4) gives

$$\frac{\sigma(R)}{R} \approx \frac{1}{D} \sqrt{(0.158)^2 + 0.01236 \left(\frac{R^2 + 4D^2}{R} \right)^2} \quad (A-5)$$

$$K_{OPT} = \frac{3.056 \cdot 10^{-4} D^2}{0.025 + 1.53 \cdot 10^{-4} \left(\frac{R^2 + 4 D^2}{R} \right)^2}$$

Figure A-2 shows K_{OPT} as a function of range for four different ocean bottom depths. This set of curves allows an operator to easily obtain a reasonable value for K_{OPT} , given that the assumed errors are reasonably accurate. If other values of the assumed errors are known to be more accurate, they can be substituted into Eqs. (A-3) and (A-4) and another set of K_{OPT} curves as a function of range and ocean depth can be plotted for use by the TMA operator.

$\sigma(D) = 450'$, D = Ocean depth at mid-range

$\sigma(\tau) = 300'$, τ = Target depth

$\sigma(\delta) = 1^\circ$, δ = Vertical angle of signal

$\sigma(\alpha) = 1^\circ$, α = Bottom slope at signal reflection point

$\sigma(B) = 1^\circ$, B = Azimuthal angle of signal

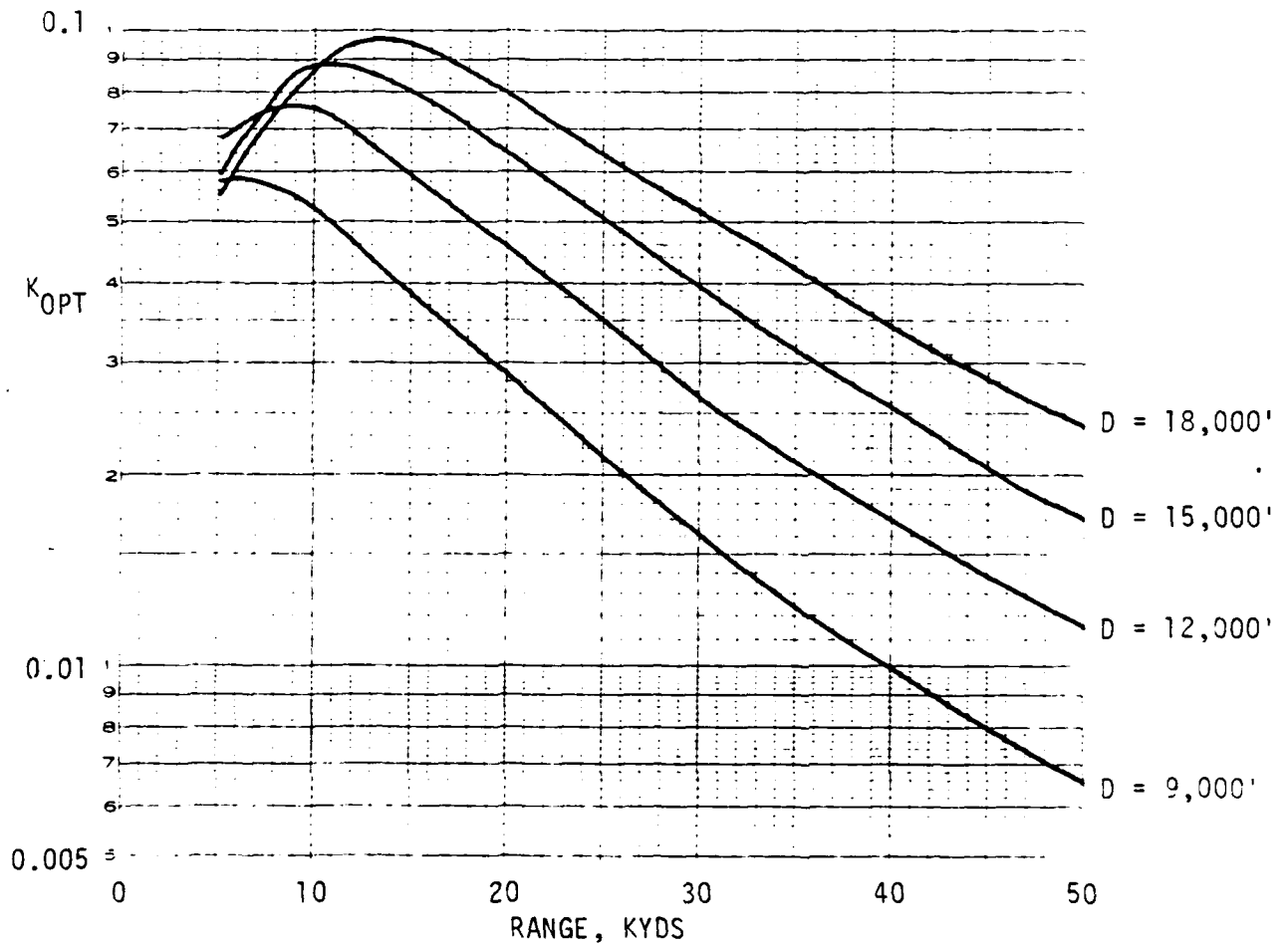


Figure A-2. K_{OPT} Versus Range and Ocean Depth.

APPENDIX B

LEAD-LAG VERSUS LAG-LEAD PLATFORM TACTICS

Bearings-only, (B - 0), TMA solution errors are known to be dependent upon the geometry of the target and platform motion. The (B - 0) TMA algorithm is based upon the assumptions: (1) that the target speed and heading (i.e., velocity) are constant throughout the solution time interval and (2) that the platform maneuvers (i.e., changes speed, heading or both) at least once during the solution time interval. It has been shown that the most accurate TMA solution for a given platform speed and solution time interval is obtained when the platform conducts a lead-leg followed by a turn and then a lag-leg of motion (i.e., a lead-lag tactic).¹ A lead-leg of platform motion is defined as one in which the platform moves in the same cross-range direction as the target, and a lag-leg is one in which the platform moves in the opposite cross-range direction.

An example will be used to show why the lead-lag tactic gives more accurate range estimates than the lag-lead tactic. Figure B-1 shows three TMA run geometries: one in which the target is moving cross-range at the same speed as the platform and the platform is conducting a lead-lag tactic; another in which the target motion is the same as the first run, but the platform is conducting a lag-lead tactic; and one in which the target is stationary and the platform conducts the same two-leg tactic as either of the first two run geometries (since, by symmetry, they are equivalent for a stationary target). The target range is about twelve times the length of each leg of platform motion for all three run geometries (i.e., $R \gg L = V_p T$).

¹McQuitty, J. M. and Gold B. A., Error Analysis of Bearings-Only TMA, Naval Surface Weapons Center, NSWCTR 81-99, 6 May 1982

The TMA algorithm solves for the X and Y components of target velocity and initial position. These Cartesian coordinate solutions can be used to calculate target range at any time before, during or after the solution time interval (which for these examples is from $t = 0$ to $t = 3T$, where T is the duration of each leg of platform motion and of the turn). The TMA range error is the difference between this calculated range and the actual target range. The same analytic method as was previously described was used to obtain the standard deviation range error, $\sigma(R)$, as a function of a given standard deviation bearing measurement error for the three TMA run geometries shown in Figure B-1. The results are shown in Figure B-2 which shows relative standard deviation range error as a function of time. The $\sigma(R)$ is normalized relative to the minimum $\sigma(R)$, which is the same for all three run geometries but which occurs at different times. The minimum $\sigma(R)$ for the stationary target occurs at the midpoint ($t = 1.5T$) of the solution time interval, and the $\sigma(R)$ at the beginning and at the end of the solution time interval is twice as large. Note that the $\sigma(R)$ curves for the three run geometries are identical except for a time shift. The $\sigma(R)$ curve for the cross-range moving target is shifted in time by minus $2T$ for the lag-lead platform motion tactic and by plus $2T$ for the lead-lag platform motion tactic. This has the effect of making the lead-lag TMA range solution more accurate at a future time, $3.5T$, (or $0.5T$ after the end, $3T$, of the solution time interval) than at any time within the solution time interval. It also has the effect of making the lag-lead TMA solution range error at time $0.5T$ after the end of the solution time interval 4.6 times as large as that of the lead-lag TMA solution. The range error of the lead-lag TMA solution at the end of the solution time interval ($t = 3T$) is about 0.57 that for the stationary target TMA solution and about 0.28 that for the lag-lead TMA solution.

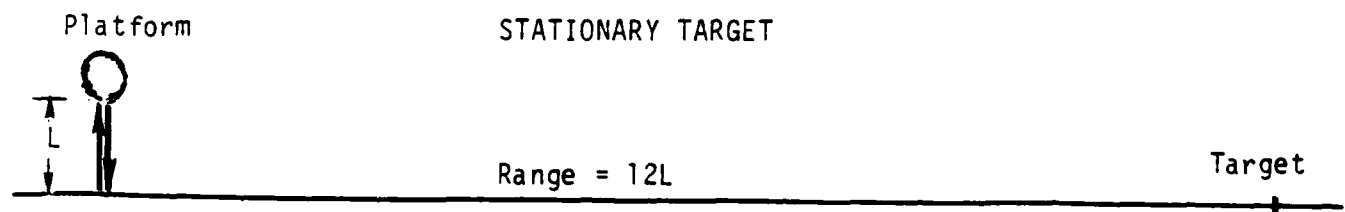
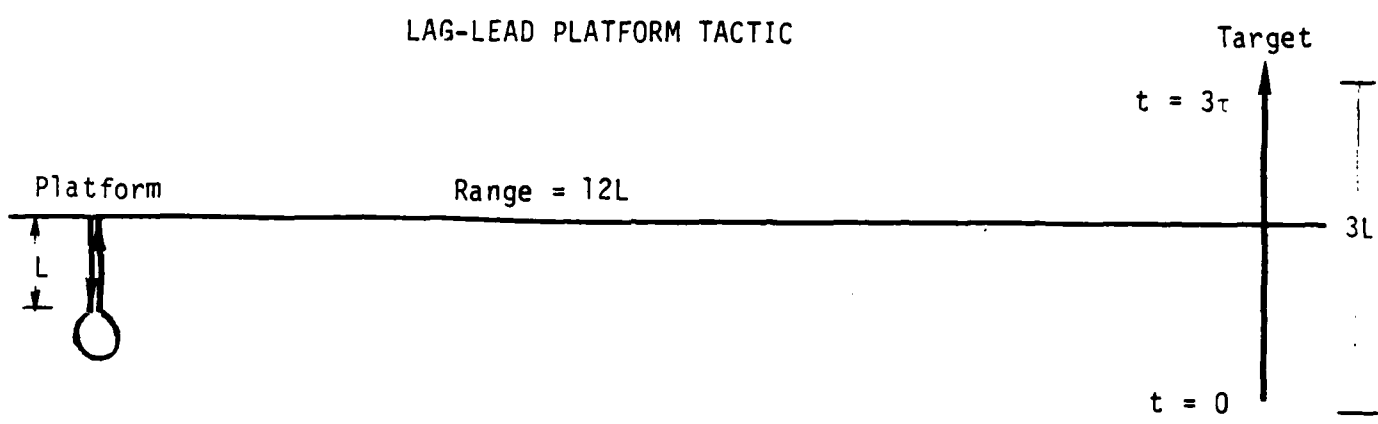
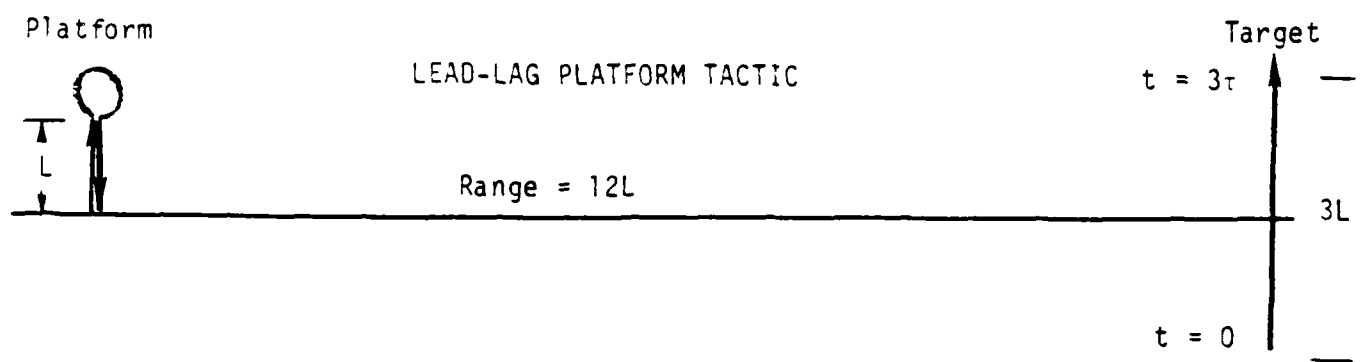


Figure B-1. Platform Target Encounter Tactics.

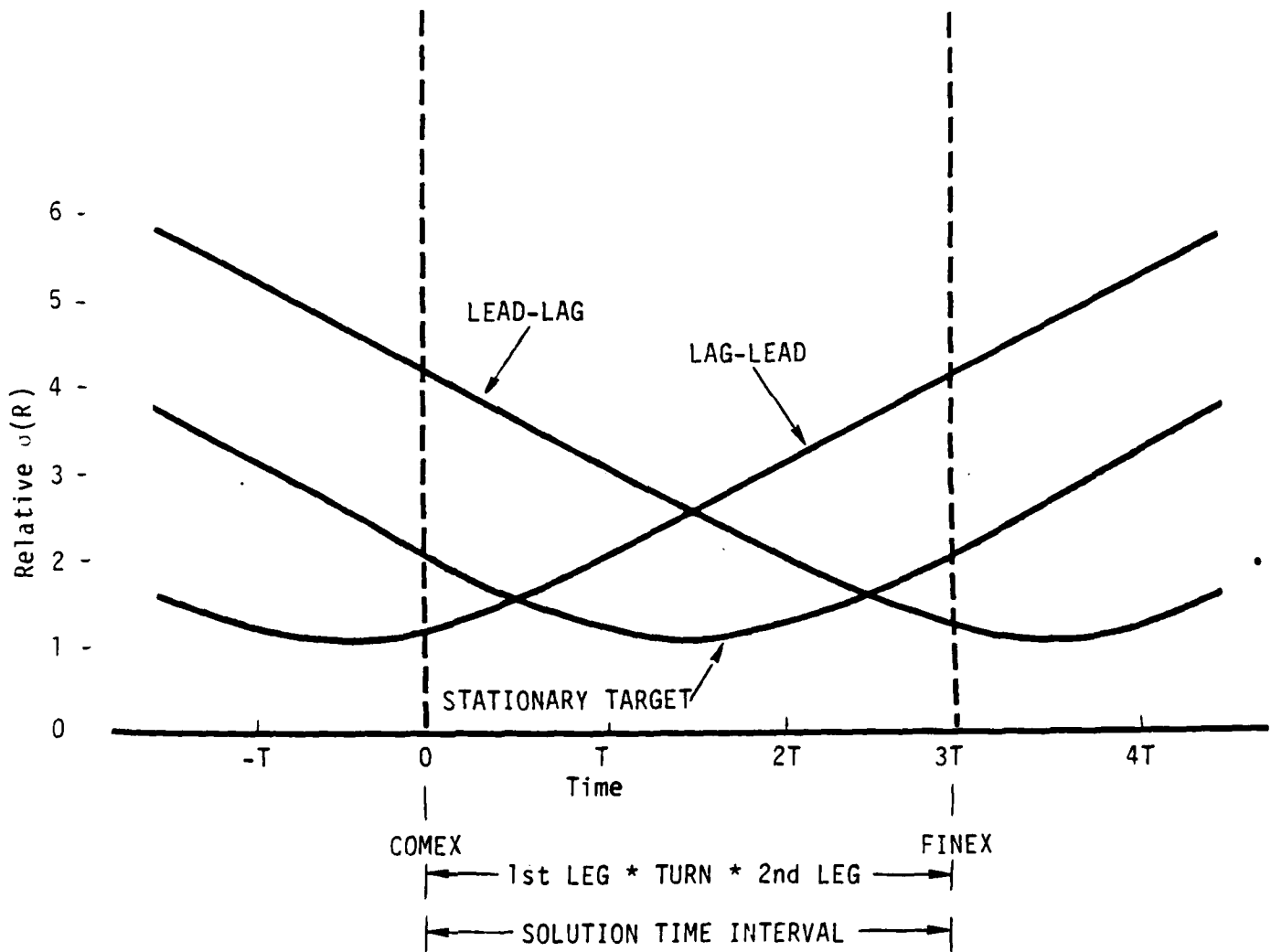


Figure B-2. Relative $\sigma(R)$ Versus Prediction Time.

If the target cross-range velocity had been greater (or less) than the platform cross-range velocity, the time displacements of the $\sigma(R)$ curves would also have been greater (or less). This example illustrates very succinctly the superiority of the lead-lag over the lag-lead platform motion tactic for all bearings-only TMA algorithms, since the difference in their accuracies is a function of the run geometry.

DISTRIBUTION LIST

	<u>Copies</u>
Chief of Naval Operations	
Attn: NOP-22T	1
NOP-224	1
NOP-353	1
NOP-951	1
Department of the Navy	
Washington, D.C. 20350	
Chief of Naval Material	
Attn: NMAT-073	1
Department of the Navy	
Washington, D.C. 20360	
Commander	
Naval Sea Systems Command	
Attn: SEA-63DB	1
SEA-63D1	1
SEA-63D41	1
SEA-63R1	1
SEA-63X1	1
SEA-63Y3	1
PMS-407C3	1
PMS-409A3	1
PMS-409A35	1
PMS-411C	1
PMS-411G	1
PMS-411E	1
Washington, D.C. 20362	
Office of Naval Research	
Attn: ONR-102	1
ONR-220	1
J. G. Smith, Code 411SP	1
800 N. Quincy Street	
Arlington, VA 22217	
Commander	
Submarine Development Squadron 12	1
Naval Submarine Base, New London	
Groton, CT 06340	

DISTRIBUTION LIST (Continued)

	<u>Copies</u>
Commander	
Naval Underwater Systems Center	
Attn: E. L. Messere	1
R. C. Chapman	1
V. J. Aidala	1
A. F. Bessacini	1
G. M. Hill	1
J. S. Davis	1
A. A. Filippini	1
K. F. Gong	1
L. Gardnier	1
N. A. Beck	1
K. Gent	1
P. Bongiovanni	1
R. Silva	1
E. Fontaine	1
B. Guimond	1
Newport, RI 20840	
Commanding Officer	
Naval Underwater Systems Center	
New London Laboratory	
Attn: A. Von Woerkom, Code 101	1
D. Harrington, Code 321	1
R. Supersano	1
J. M. Woodside	1
New London, CT 06320	
Commander	
Submarine Development Group Two	1
Naval Submarine Base, New London	
Groton, CT 06340	
Commander	
Surface Warfare Development Group	1
Norfolk, VA 23521	
Superintendent	
Naval Postgraduate School	
Attn: Technical Library	1
H. Titus, Code 62Ts	1
Electrical Engineering Department	1
Physics Department	1
Monterey, CA 93940	

DISTRIBUTION LIST (Continued)

	<u>Copies</u>
Superintendent U.S Naval Academy Attn: Technical Library Annapolis, MD 21402	1
Commander Submarine Force, U.S. Atlantic Fleet Norfolk, VA 23511	1
Commander Naval War College Newport, RI 22841	1
Commander Anti-Submarine Warfare Force, Pacific Fleet Post Office San Francisco, CA 96610	1
Commander Naval Ocean Systems Center Attn: M. J. Shensa S. I. Chou Library San Diego, CA 92152	1 1 1
Commander NAVSUBPAC Pearl Harbor, HI	1
Commander Naval Surface Weapons Center Attn: U U04 U21 (M. M. Coate) U21 (B. L. Stripling) U21 (J. Arvelo) U21 (B. A. Gold) U22 (T. B. Ballard) Library Silver Spring, MD 20903-5000	1 1 1 1 1 1 1 1
Defense Technical Information Center Building 3, Cameron Station Alexandria, VA 22314	2

DISTRIBUTION LIST (Continued)

	<u>Copies</u>
Analysis and Technology, Inc. Attn: T. M. Downie H. F. Jarvis C. B. Billings, Jr. P. O. Box 220 North Stonington, CT 06359	1 1 1
Bolt, Beranek and Newman, Inc. Attn: G. Sheppard 10 Moulton Street Cambridge, MA 02238	1
Raytheon Company Attn: R. Lamp 1847 West Main Road P. O. Box 360 Portsmouth, RI 02871	1
IBM Corporation Attn: G. W. Johnson 9500 Godwin Drive Manassas, VA 22110	1
University of Rhode Island Attn: Department of Electrical Engineering Department of Mathematics Kingston, RI 02881	1 1
Virginia Polytechnic Institute and State University Attn: Department of Electrical Engineering (R. Moose) Blacksburg, VA 24061	1
Massachusetts Institute of Technology Attn: N. Sandell, Room 35-213 Cambridge, MA 02139	1
Sperry Gyroscope, Sperry Rand Corporation Attn: F. Brenner (Micropuffs Project) Marcus Avenue Great Neck, NY 11020	1
Yale University Attn: P. M. Schultheiss, Electrical Engineering Department New Haven, CT 06520	1